DNMI - RAPPORT

NORWEGIAN METEOROLOGICAL INSTITUTE
BOX 43 BLINDERN , N - 0313 OSLO

PHONE +47 22 96 30 00

ISSN 0805-9918

REPORT NO.
10/01 KLIMA

DATE
10.10.01

TITLE Precipitation scenarios for Norway
Empirical downscaling from the ECHAM4/OPYC3 GSDIO integration

AUTHORS

I. Hanssen-Bauer, O.E. Tveito and E.J. Førland

PROJECT CONTRACTORS
Norwegian Research Council (Contract no 120656/720) and Norwegian Meteorological institute.

Abstract

The 2m temperature and the SLP field from the ECHAM4/OPYC3 GSDIO integration (which includes effects of greenhouse-gases and tropospheric ozon, as well as direct and indirect effects of sulphur aeroseols) were used as predictors for empirical downscaling of local monthly precipitation over Norway during the period 1870-2050. Temperature was used as predictor in addition to the SLP-field because it is crucial to include a predictor which carries the greenhouse signal. The use of temperature as an additional predictor gave improved results in autumn, winter, and partly during spring. In summer, however, it led to physically suspect results, and temperature was thus skipped as predictor for the summer months.

The empirically downscaled precipitation series indicate an increase in the average annual precipitation of 0.3 to 2.7 % per decade during the coming 50 years at the Norwegian mainland, and about 1.5 % per decade on Svalbard. The projected increase rates are generally smallest in south-eastern Norway, where they are not statistically significant (5% level) and largest along the north-western and western coast, where they are highly significant. In winter, statistically significant positive trends (+1.8 to 3.2 % per decade) are found all over the country. The largest increase rates are found in southern Norway. Also in autumn, the precipitation increase (+0.6 to 5.9 % per decade) is statistically significant at most places. The largest autumn increase rates are found in western and north-western regions. The modelled increase in winter- and autumn precipitation is, all over the country, partly accounted for by the temperature increase. In the regions where the largest precipitation increases are found, however, at least half the increase is attributed to changes in the atmospheric circulation. Modelled spring precipitation tends to decrease in southern Norway and increase in northern Norway. These changes are statistically significant only in two northern regions and on Svalbard. Modelled summer precipitation tends to decrease in eastern areas and increase in western areas, but the changes, which are entirely attributed to changes in the atmospheric circulation, are statistically significant only in 6 of 14 regions.

The above results mainly agree with the precipitation scenarios that were calculated by dynamical downscaling from the same global scenario. An exception is found during summer, when dynamical downscaling tends to project significant precipitation increase in larger areas.

SIGNATURE

.....	.....
Eirik Førland	Bjørn Aune
Principal Investigator, RegClim-PT3	Head of the Climatology Division

Precipitation scenarios for Norway

Empirical downscaling from the ECHAM4/OPYC3 GSDIO integration

Contents

Foreword

The present report is a result from the project “Regional climate development under global warming” (RegClim) (Iversen at al.1997), which is supported by the Norwegian Research Council (NRC Contract No 120656/720). The work is done within the frames of Principal Task 3 “Empirical Downscaling”.

1. Introduction

One of the overall aims of the RegClim project (Iversen at al.1997) is to estimate probable changes in the climate in Norway, including Svalbard, under global warming. Coupled atmospheric-ocean global general circulation models (AOGCMs) are the most sophisticated tools for modelling global warming. The resolution in the recent AOGCMs is probably sufficient for modelling large-scale features, but in general still too coarse to enable these models to reproduce the climate on regional or local scale (Figure 1). It is thus a need for downscaling of the results from the AOGCMs.

Within the RegClim project, we have approached this problem both applying dynamical and empirical downscaling techniques (e.g. Murphy 1999). In both approaches, we have mainly been working with the results from the Max-Planck-Institute's AOGCM, ECHAM4/OPYC3 (Roeckner et al., 1996, 1998, 1999), and mainly with the "GSDIO" integration which is a transient integration including greenhouse gases, tropospheric ozon, and direct as well as indirect sulphur aerosol forcing (Roeckner et al. 1999). Results from the dynamical downscaling experiments were reported by Bjørge et al. (2000). Results from empirical downscaling of temperature and precipitation based upon several global models were reported by Benestad (2000). Hanssen-Bauer et al. (2000) presented temperature scenarios resulting from empirical downscaling of temperatere in Norway including Svalbard based upon the GSDIO integration only. In the present report, similar scenarios for precipitation will be presented and compared to the results from the dynamical downscaling.

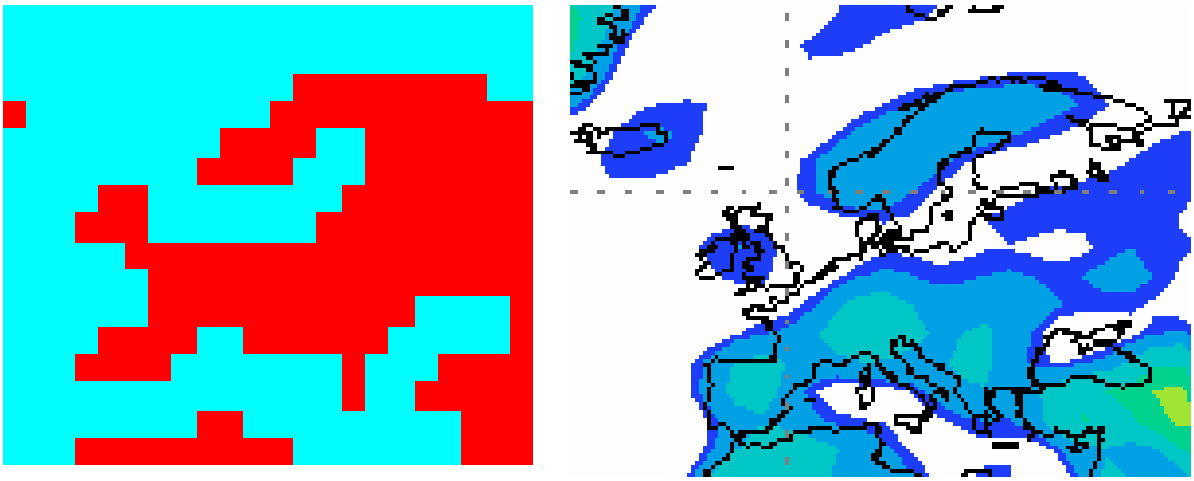

Figure 1. Land-mask (left) and topography (right) for the ECHAM4/OPYC3 GSDIO integration.

2. Methods and data

"Empirical downscaling" denotes methods involving the use of empirical links between large-scale fields (predictors) and local variables (predictands) to deduce estimates of the local variables from the large-scale fields. Surveys of methods for establishing such links are given by Hewitson and Crane (1996), Wilby and Wigley (1997) and Zorita and von Storch (1997, 1999). Both linear techniques (multivariate regression, singular vector decomposition, canonical correlation) and non-linear ones (analogue techniques, weather classes, neural networks) have been applied. The optimal choice of method depends highly on the choices of predictors, predictands, and also the time resolution. On a monthly basis, both linear and non-linear techniques may usually be applied.

2.1 Predictands and predictors

In the present work, the predictand is local monthly precipitation at selected Norwegian stations (Fig. 2). Table A1 (Appendix) gives geographical coordinates and other relevant information for these stations. Hanssen-Bauer and Førland (1998) concluded that when precipitation is given in per cent of the 1961-1990 average ("standard normal"), the variation at the Norwegian mainland during the last 100 years is described fairly well by monthly series from 13 "precipitation regions". The absolute precipitation may vary by a factor of 10 within a specific region, but there is high correlation between precipitation series from different stations within the region. Svalbard is defined as region 14. Note, however that this region includes only stations situated at the west coast of the island Spitsbergen (Fig. 2), and that the results for this region thus are valid only for this part of the archipelago.

Because of the high correlation within the regions, it is actually the 14 standardised regional series, *SR*, that are used as predictands in the present study. The precipitation *R* for a specific locality *x* in region *m* is then estimated by:

$$R_{xm}(t) \approx SR_m(t) \cdot SN_x/100 \qquad (1).$$

Here, $SR_m(t)$ is the regional precipitation series for region *m* given in %, and SN_x is the 1961-1990 precipitation standard normal for station *x*.

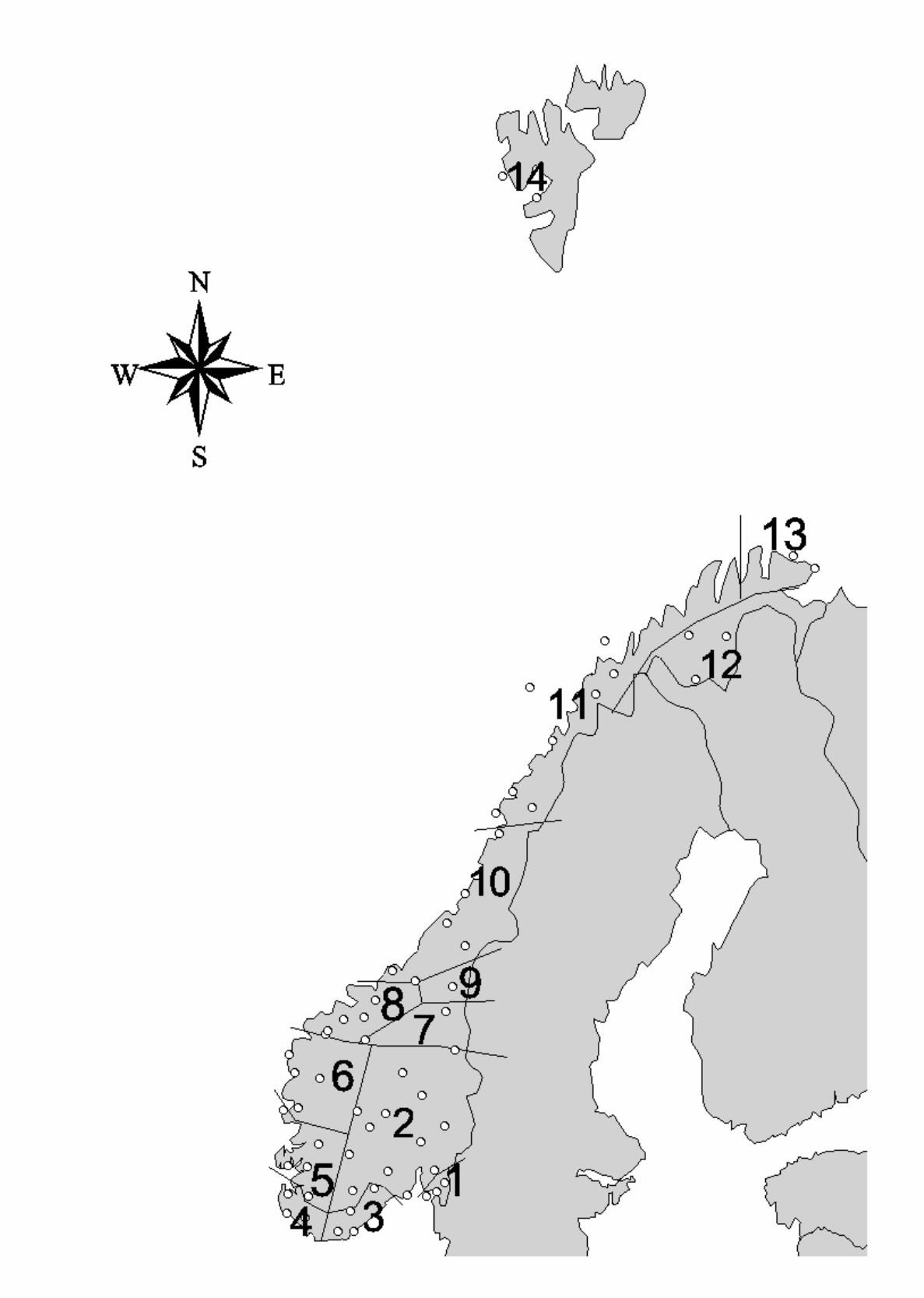

*Figure 2. Precipitation regions 1-14 and stations (**o**) used in the present paper.*

The optimal choice of predictors is dependent on the predictands, but also on the specific problem. When applied for making local climate scenarios from AOGCM global warming scenarios, at least three conditions should be fulfilled:

1. The large-scale fields which are used as predictors should be realistically modelled by the AOGCM;
2. The links between the predictors and the local predictands should be strong and robust, i.e. the predictors should account for a dominant part of the variance in the predictands, and the links should be stable in time;
3. At least one of the predictors should carry the "global warming signal".

A commonly used predictor for downscaling local climate is the sea level pressure (SLP) field. This is partly because there exist long global series of gridded SLP, but also because the AOGMCs generally reproduce the main features of the SLP field reasonably well (cf. condition 1 above). Hanssen-Bauer and Førland (2001) showed that the average SLP field from the ECHAM4/OPYC3 GSDIO integration has a bias over Norway. However, as the anomalies from the average field are fairly realistic, one may adjust for this bias, simply by using the anomaly field as predictor rather than the field itself.

Another reason for the widespread use of the SLP field in downscaling studies is that investigations from several locations have shown that it is possible to find robust empirical links between SLP fields and local precipitation and temperature (e.g. Werner and von Storch 1993, Zorita et al. 1995, Hanssen-Bauer and Førland 1998) (cf. condition 2 above). Specificly, Hanssen-Bauer and Førland (2000) demonstrated that variations in the large-scale SLP field over the northern North Atlantic and Europe account for most of the long-term trends and decadal scale variability we have seen in Norwegian precipitation series the last 100 years. However, exceptions are found in eastern parts of the country, especially for winter precipitation, indicating that some of the precipitation variation is not connected to changes in the SLP field. It is thus concluded that at least one additional predictor is needed to model precipitation. This is in accordance with Wilby and Wigley (2000), who investigated several possible predictors for downscaling precipitation, and concluded that multivariate prediction equations are essential in order to produce high quality downscaling schemes for precipitation. They found that, in addition to circulation related variables, specific humidity seems to be a promising predictor. As the humidity field from the GSDIO integration has not been validated and the quality of the observations of humidity has not been checked, we are still reluctant to apply this variable as a predictor. Instead, we have chosen to use 2m temperature (T) as a proxy for atmospheric moisture content. Wilby and Wigley (2000) showed that the correlation between daily specific humidity and temperature (especially minimum temperature) is good. Using T as a predictor also ensures that the global warming signal is included (Crane and Hewitson 1998) (cf. condition 3 above).

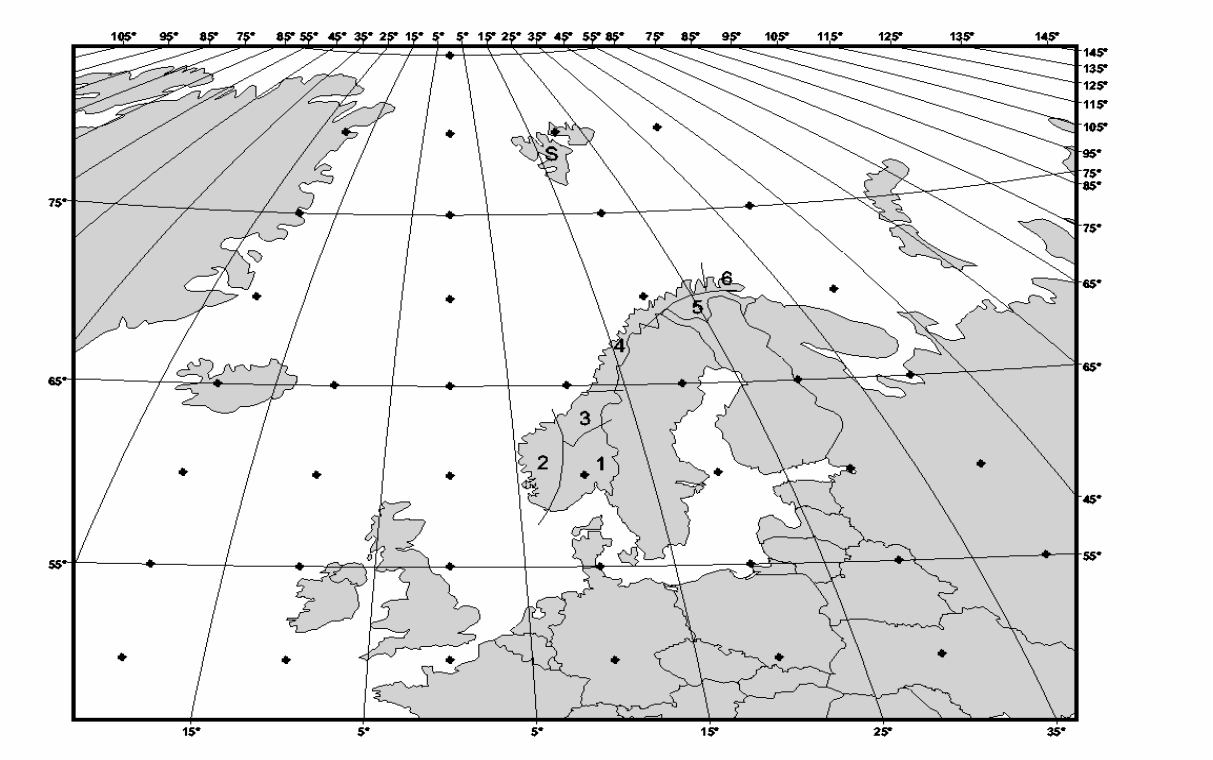

Figure 3. Predictor areas: SLP gridpoints (+) and temperature regions(1-6 at the Norwegian mainland, S at Svalbard).

The choice of "predictor area" has been proved to affect the results of empirical downscaling (e.g. Benestad 2001). Wilby and Wigley (2000) found that the optimal choice of predictor area is dependent of the predictor: While maximum correlation between SLP and precipitation often occurred away from the locality where the precipitation was investigated, the correlation between humidity and precipitation was at maximum when the data were propinquitos. In the present study, different areas are thus used for SLP and T (Fig. 3). For SLP, the area 20°W-40°E, 50-85°N was applied. This was also applied by Hanssen-Bauer and Førland (2000) for assessing the empirical links between SLP and local climate. For temperature on the other hand, only a standardised temperature representative for the actual region is applied. Temperature regions in Norway were defined by Hanssen-Bauer and Nordli (1998) and applied by Hanssen-Bauer et al.(2000) for empirical downscaling of temperature. The temperature regions are, as the precipitation regions, characterised by highly correlated variation rather than homogeneous climate conditions. For each precipitation region, the standardised temperature from one of the temperature regions is used as a predictor (Table 1).

Table1. Predictors for precipitation in different precipitation regions.
"SLP"is SLP from the grid-points shown in Fig. 3. "ST" is standardised temperature in the temperature region indicated by the index..

Precip.Reg.	1	2	3	4	5	6	7	8	9	10	11	12	13	14
Predictors	SLP and ST_1	SLP and ST_1	SLP and ST_1	SLP and ST_2	SLP and ST_2	SLP and ST_2	SLP and ST_3	SLP and ST_3	SLP and ST_3	SLP and ST_3	SLP and ST_4	SLP and ST_5	SLP and ST_6	SLP and ST_S

Table 2. Eigenvalues of the covariance matrix in the common EOF analysis.
Second row shows the difference between the eigenvalue of the current EOF and the next.
Last row shows the cumulative proportion of the variance accounted for by the leading EOFs

	EOF1	EOF2	EOF3	EOF4	EOF5	EOF6	EOF7	EOF8	EOF9	EOF10	EOF11	EOF12
Eigenvalue	594	308	268	77	65	42	13	11	9	6	4	3
Difference	286	40	191	12	23	29	2	2	3	2	1	-
Cum. Prop. of variance	.42	.64	.83	.88	.93	.96	.97	.98	.98	.98	.99	.99

The monthly standardised regional temperature series are used as predictors directly: For historical conditions the time series calculated by Hanssen-Bauer and Nordli (1998) are applied; for the GSDIO integration the regional series downscaled by Hanssen-Bauer et at. (2000) are applied. For SLP the monthly gridded fields from the UK Met Office and the monthly averaged output from the GSDIO integration are applied to represent historical and modelled climate, respectively. These fields are not used directly, but rather their "common EOFs" (Benestad 2001). The 6 leading common EOFs are applied as they include 96% of the variance, and there is a gap between the 6^{th} and 7^{th} EOF (Table 2).

2.2 Downscaling model development

Downscaling models were developed by multiple regression based upon historical data during the period 1900-1960, while data from the period 1961-1998 were used for validation. Models were developed for each precipitation region and for each calendar month separately. Two sets of models were developed: One set where only the 6 leading EOFs from the SLP-field were predictor candidates, and one where also the regional temperature was included. In the models involving SLP only, stepwise regression was applied in order to exclude EOFs that did not significantly improve the model. A significance level of 0.15 was used for entry of new components. In the models involving also temperature, temperature was used as predictor in addition to the EOFs that were included by the stepwise regression. The reason for not allowing the stepwise procedure to exclude temperature is that, even if temperature may not appear to be the most significant predictor in a stable climate, the changes in this predictor in the future may be critical for determining the change in precipitation. This aspect was discussed thoroughly by IPCC (2001) in chapter 10.

Table 3 shows examples of correlation between observed and modelled precipitation during the training period and the validation period, both for models including T as a predictor and for models where only the SLP field is applied. There is no systematic difference between training period and

Table 3. Correlation coefficients between observed and modelled precipitation during the training and validation period. Results are given on seasonal basis for the stations Bjørnholt in region 2, Samnanger in region 6, Drevja in region 10 and Svalbard Airport in region 14.

Station	Period	Models including T				Models without T			
		WIN	SPR	SUM	AUT	WIN	SPR	SUM	AUT
Bjørnholt	1900-1960	0.88	0.68	0.79	0.84	0.84	0.68	0.75	0.84
	1961-1998	0.77	0.74	0.80	0.82	0.64	0.74	0.75	0.82
Samnanger	1900-1960	0.91	0.89	0.73	0.91	0.90	0.88	0.68	0.89
	1961-1998	0.93	0.89	0.84	0.88	0.93	0.87	0.81	0.88
Drevja	1900-1960	0.91	0.77	0.61	0.89	0.89	0.77	0.59	0.88
	1961-1998	0.92	0.81	0.64	0.90	0.90	0.80	0.63	0.88
Svalbard Airport	1900-1960	0.45	0.64	0.67	0.56	0.42	0.61	0.65	0.53
	1961-1998	0.38	0.73	0.66	0.51	0.35	0.70	0.64	0.48

validation period. On the Norwegian mainland, the correlation coefficient between observed and modelled precipitation in spring and autumn improves only marginally by inclusion of temperature. In eastern Norway ("Bjørnholt" in Table 3) the model including T is better during winter, especially during the validation period 1961-1998. Also during summer, the model including T tends to be slightly superior. This is illustrated by Figure 4, which shows low pass filtered precipitation series (observed and modelled) for the stations in region 2 and 6, respectively.

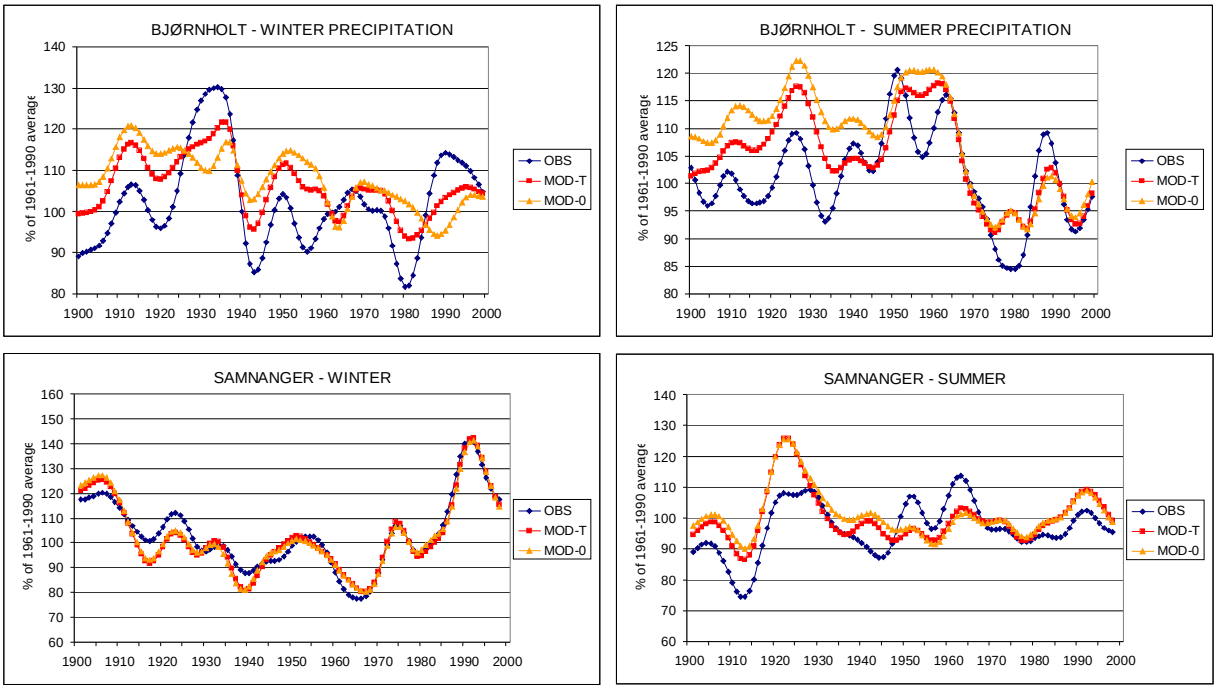

Figure 4. Winter (left) and summer (right) precipitation series at two Norwegian stations. Observed series (blue) are shown together with modelled series with (red) and without (yellow) temperature as predictor. The series are filtered in order to show decadal scale variability. Upper panels: "Bjørnholt" in region 2 in eastern Norway. Lower panels: "Samnanger" in region 6 in western Norway.

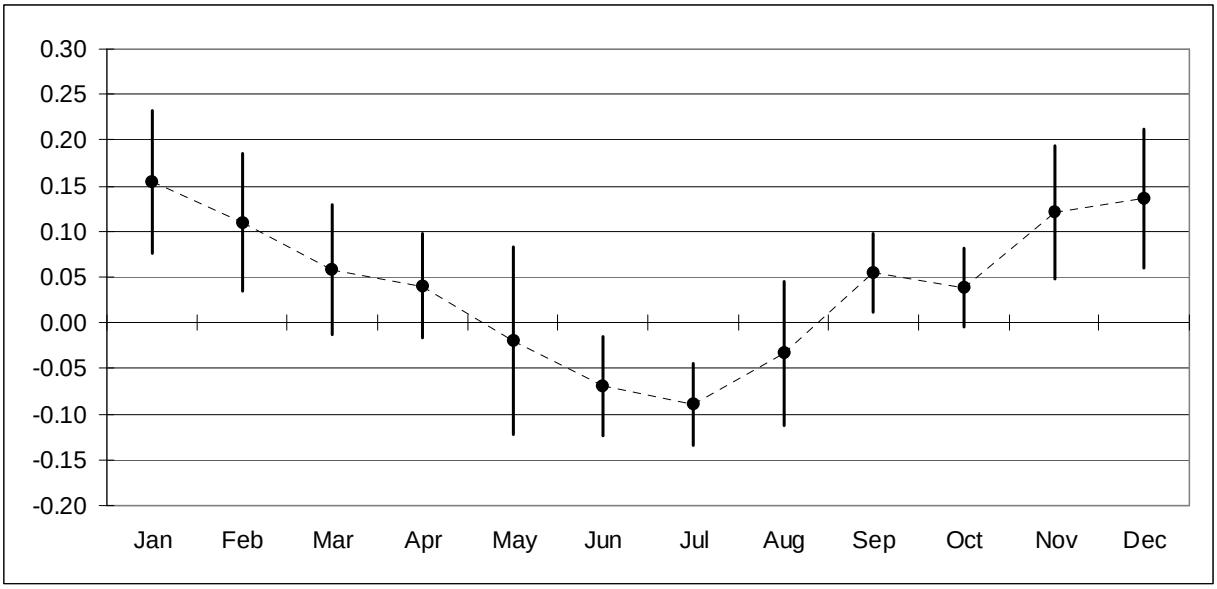

Figure 5. Regression coefficients for standardised temperature in the precipitation regression equations: Averages and standard deviations for the 14 regions.

In the regression equation temperature is used as a proxy for air humidity. The physical background for this is that warm air potentially can carry more precipitable water than cold air. Wilby and Wigley (2000) showed from observations over the U.S.A. that there is a correlation of about 0.8 between daily minimum temperature and specific humidity both during summer and winter. For daily maximum temperature the correlation is 0.7 in winter and 0.3 in summer. The regression coefficient is thus expected to be positive when using temperature as a predictor for precipitation. Figure 5 shows, on the other hand, that the regression coefficient for the temperature term has a distinct annual variation, and it is negative during the summer months. The reason for this is probably that air humidity is not the only link between temperature and precipitation, and in summer, when the connection between temperature and humidity is weakest (cf. the results from Wilby and Wigley 2000), other links may dominate. A possible additional link is connected to cloud cover: Precipitation is associated with heavy cloud cover. In winter the average clear-sky radiation balance at the ground is often negative, and clouds tend to decrease the radiation loss from the ground and thus increase the temperature. In summer, on the opposite, clouds mainly reduce the positive net radiation at the ground and thus tend to reduce the temperature. The temperature-cloud-precipitation link may thus explain the seasonal variation, and specifically the negative regression coefficients during summer.

When validating predictands for use in climate change studies, it is crucial to discuss the physical mechanisms behind the empirical links that are found, and to assess whether it is likely that they will persist in a changed climate. The connection between temperature and air humidity is probably valid also for the future warming: The hydrological cycle will be intensified because of the global warming. The connection between temperature and cloud cover, however, is less likely to be valid for the

greenhouse warming: The future warming is not primarily a response to changes in the cloudiness. This warming will thus probably not be connected to changes in cloud cover in the same way as the empirical links prescribe. When downscaling the future precipitation changes from temperature, we would thus like to include the changes which are connected to changes in humidity, but not those connected to changes in cloud cover. The problem is that it is not possible to distinguish between them: It is their combined effect that is detected by the empirical methods. Wilby and Wigley (2000), however, conclude that though specific humidity is a reasonably good predictor for precipitation during winter, it is a poor predictor during summer. As T in the present study is used as a proxy for humidity, this is an argument for not applying T as a predictor for precipitation during the summer months.

In the present study, we have thus chosen the following solution: EOFs from the SLP field are applied as predictors for precipitation in all calendar months, while T is applied as an additional predictor only for months where the regression coefficient is positive. In southern regions, this is usually September through April, while it is September through May on Svalbard. The modelled precipitation changes in summer will then with few exceptions result only from the changes in the atmospheric circulation. This is not ideal, but at least better than using a predictor which seems dubious as an indicator of the "greenhouse signal". During the rest of the year, the modelled precipitation changes result both from circulation changes and from temperature changes. In winter, the modelled precipitation increase which results from the temperature increase may be exaggerated because the effect from the "temperature-cloudiness-precipitation" connection is included and it is positive during winter. In autumn and spring, on the other hand, the total effects from this connection is probably close to zero.

2.3 Validation of the downscaling models

Downscaling models were developed separately for the 14 precipitation regions. The best fit was achieved in the westerly region 6, while the poorest fit was achieved in the Arctic region 14. Filtered series of observed and modelled seasonal precipitation from one station in each of these regions are shown in Figure 6. Though the correlation coefficients between observed and downscaled seasonal precipitation at Svalbard Airport are rather poor (cf. Table 3), most of the decadal scale variability (except in winter) is reproduced by the downscaling models even here.

A disadvantage by using linear downscaling techniques is that, even though long-term averages and trends may be modelled satisfactorily, the variance of the predictand generally is reduced by the

Table 4. Standard deviations for observed and modelled seasonal precipitation during the periods 1931-1960 and 1961-1990. Results are given for winter, spring, summer and autumn, for the stations Bjørnholt in region 2, Samnanger in region 6, Bones in region 11 and Svalbard Airport in region 14. Unit: % of the 1961-1990 average

STATION	DATA	PERIOD	WIN	SPR	SUM	AUT
Bjørnholt (Reg. 2)	OBS	1931-1960	46	33	38	29
		1961-1990	41	35	34	36
	DOWN-SCALED	1931-1960	36	20	33	27
		1961-1990	29	25	27	25
Samnanger (Reg. 6)	OBS	1931-1960	33	38	23	29
		1961-1990	40	41	30	26
	DOWN-SCALED	1931-1960	30	31	16	27
		1961-1990	43	36	18	19
Bones (Reg. 11)	OBS	1931-1960	43	49	20	31
		1961-1990	37	33	33	37
	DOWN-SCALED	1931-1960	32	32	19	27
		1961-1990	31	31	19	30
Svalbard Airport (Reg. 14)	OBS	1931-1960	50	30	34	41
		1961-1990	40	46	44	30
	DOWN-SCALED	1931-1960	32	28	25	18
		1961-1990	25	38	22	20

model. Table A2 in Appendix shows, for 4 different stations, averages and standard deviations of observed and modelled seasonal precipitation over different 30-year periods. The standard deviations for two of these periods are also given in Table 4. The reduction in standard deviations is at maximum at Svalbard Airport, where the correlation coefficient between observed and modelled precipitation is at minimum, while it is small at Samnanger, where most of the variance is accounted for by the model. This indicates that the statistical distribution of the downscaled seasonal precipitation values is more realistic at Samnanger than at Svalbard Airport. This is confirmed by Figure 7: At Samnanger the similarity between observed and modelled cumulative frequency distributions is far better than Svalbard Airport.

The downscaling models tend to have problems with reproducing the observed frequencies of seasons with more than about 170% of “normal” precipitation. At Svalbard, this tendency is seen in all seasons, while we mainly can see it in winter and spring at Samnanger. The models also tend to underestimate the frequency of seasons with less than 50% of “normal” precipitation, especially in summer. When the downscaling models are used for producing scenarios, one should keep in mind this inability to reproduce extremely high or low amounts of precipitation.

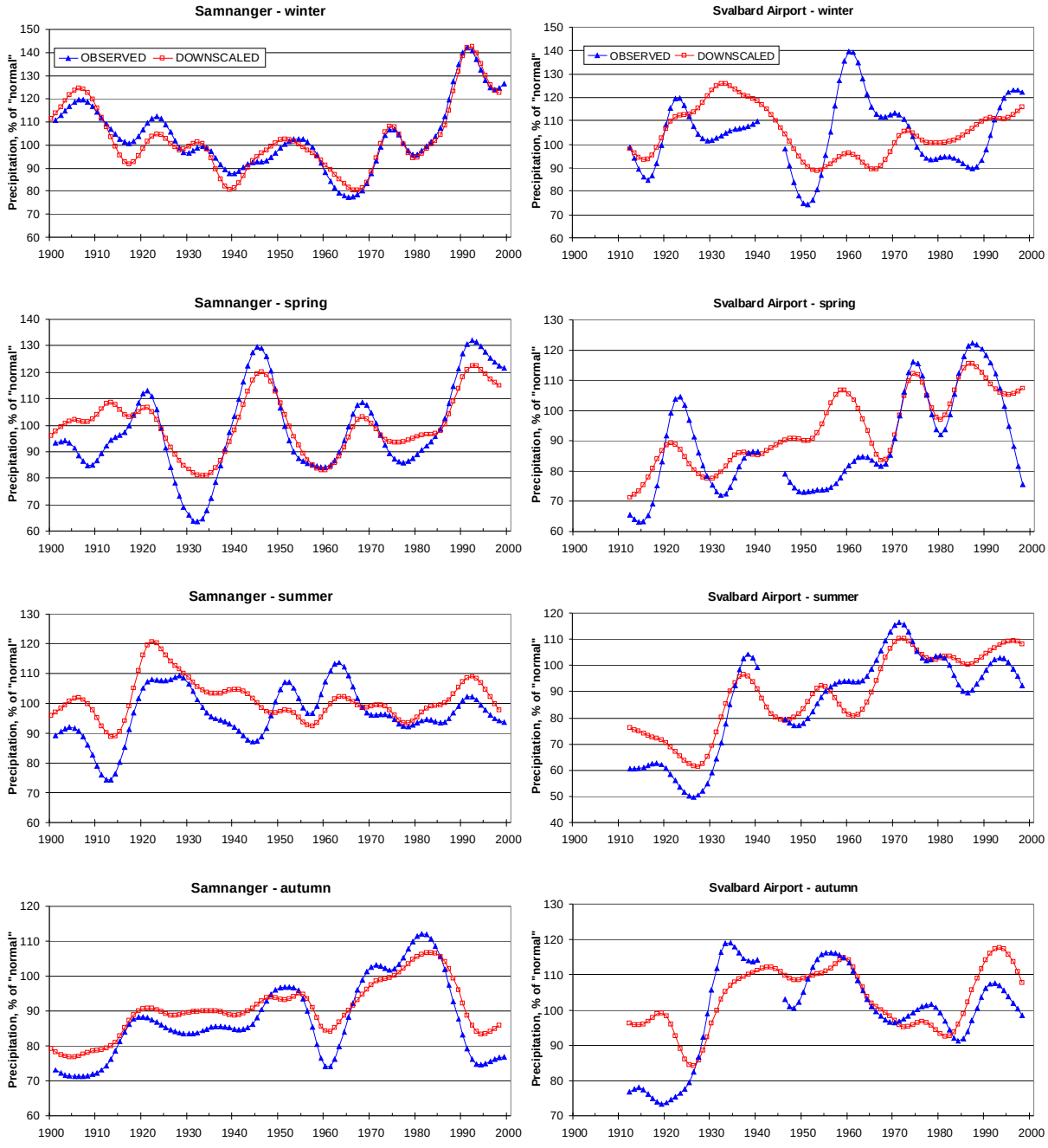

Figure 6. Filtered series of observed (blue) and downscaled (red) seasonal precipitation at the stations Samnanger (left) and Svalbard Airport (right).

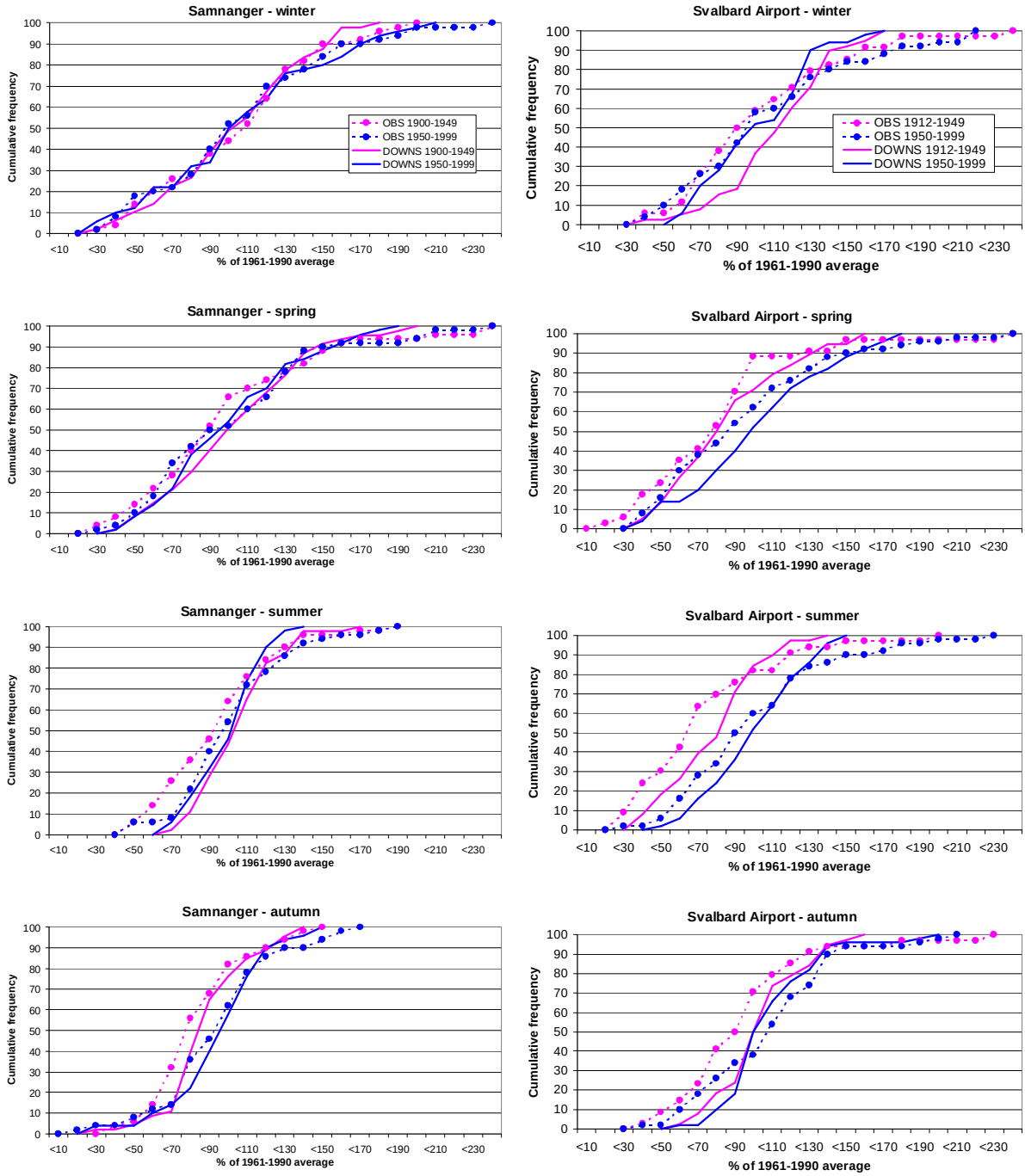

Figure 7. Cumulative frequency distributions of observed (--•--) modelled (——)seasonal precipitation at the stations Samnanger (left) and Svalbard Airport (right) for 2 different periods.

3. Results: Downscaling of the GSDIO integration

The downscaling models were applied on the output from the ECHAM4/OPYC3 GSDIO integration in order to produce monthly precipitation scenarios for the 14 precipitation regions. In order to make site-specific scenarios, the regional scenarios were multiplied by the stations' 1961-1990 averages. The following results are presented on seasonal basis.

3.1 Frequency distributions

The results from the empirical downscaling of precipitation from the GSDIO integration may to a certain degree be evaluated by comparing values from the period 1900 to 2000 to downscaling results based upon observations from the same period. The comparison cannot be done on a year-to-year basis, as natural inter-annual variability is not in phase in model and reality. It is thus the statistical properties that should be compared. In the present report, this is done by comparing frequency distributions of seasonal precipitation sums during different 50-year periods at selected stations (Figures 8-11). The frequency distribution for the period 2000-2049 is included for the GSDIO integration.

In most cases, the frequency distributions of precipitation downscaled from the GSDIO integration during the 20th century are quite similar to the corresponding downscaling results based upon observations. Systematic differences are found in summer in south-eastern Norway (Figure 8) where the GSDIO tends to give to few cases with precipitation above the 1961-90 average, and in autumn in north-western Norway (Figure 10) where the GSDIO gives too many cases with precipitation above the 1961-90 average. At Svalbard (Figure 11), the frequency distributions from the downscaled GSDIO integration fits well with the 1950-1999 observation based frequency distribution. However, the GSDIO integration does not reproduce the increase which is seen in spring and summer precipitation from the first to the second half of the 20th century.

Concerning precipitation changes from the 20th century to the first part of the 21st century, the contrasts between different parts of the country are larger than for temperature. At the Norwegian mainland (Fig. 8 - 10), the downscaled GSDIO results generally give increased precipitation in autumn and winter. In south-western regions, increased summer precipitation is also projected, while south-eastern regions according to this scenario gets less summer precipitation. The main feature at Svalbard (Fig. 11) is the projected increase in spring precipitation. No tendency is found indicating that the increase in extremely wet seasons will exceed the general precipitation increase.

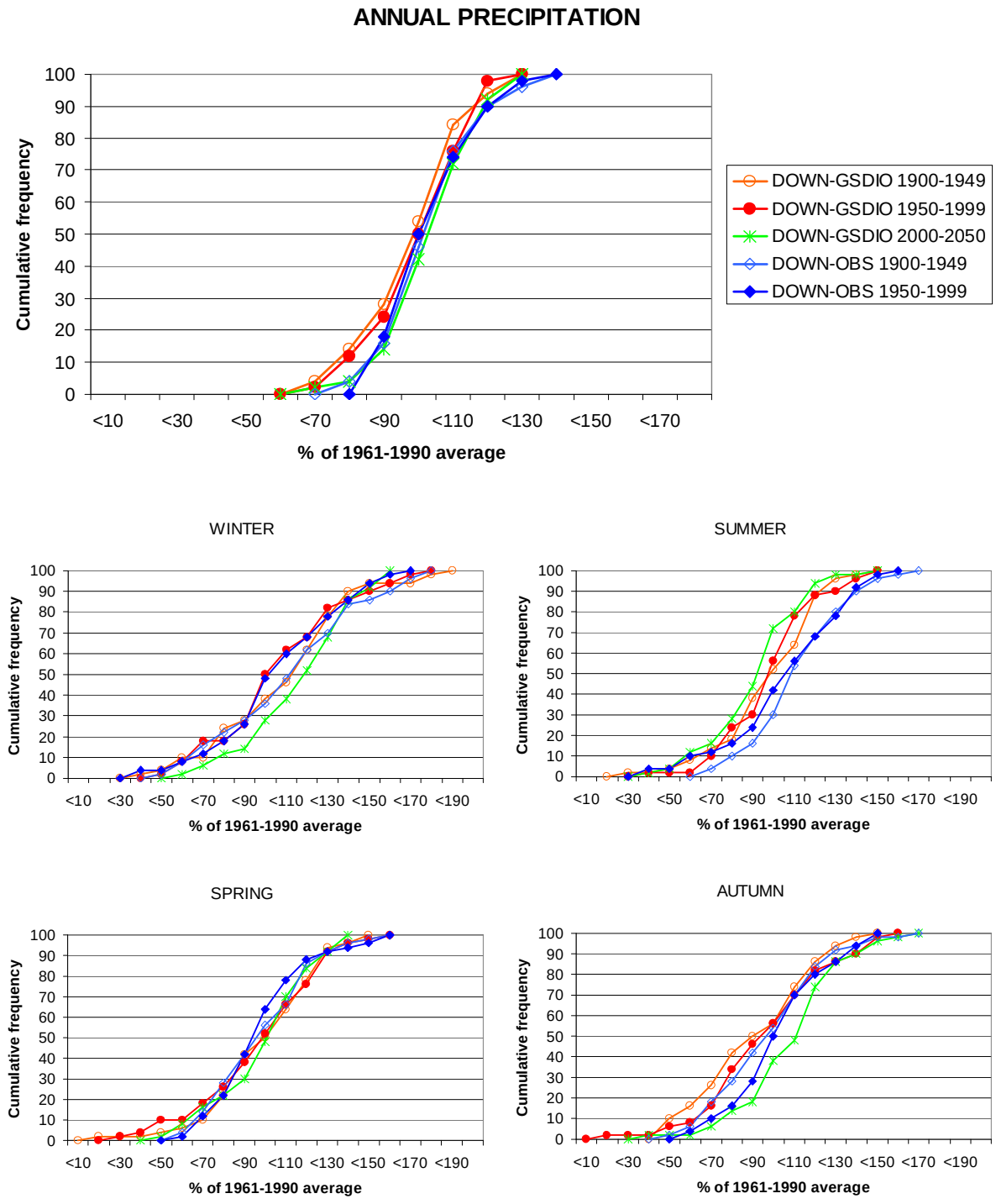

Figure 8. Cumulative frequency distributions of downscaled precipitation during the 20th century from observations (blue) and the GSDIO integration (red) at Bjørnholt in region 2. Downscaled GSDIO scenario for the period 2000-2049 is also shown (green).

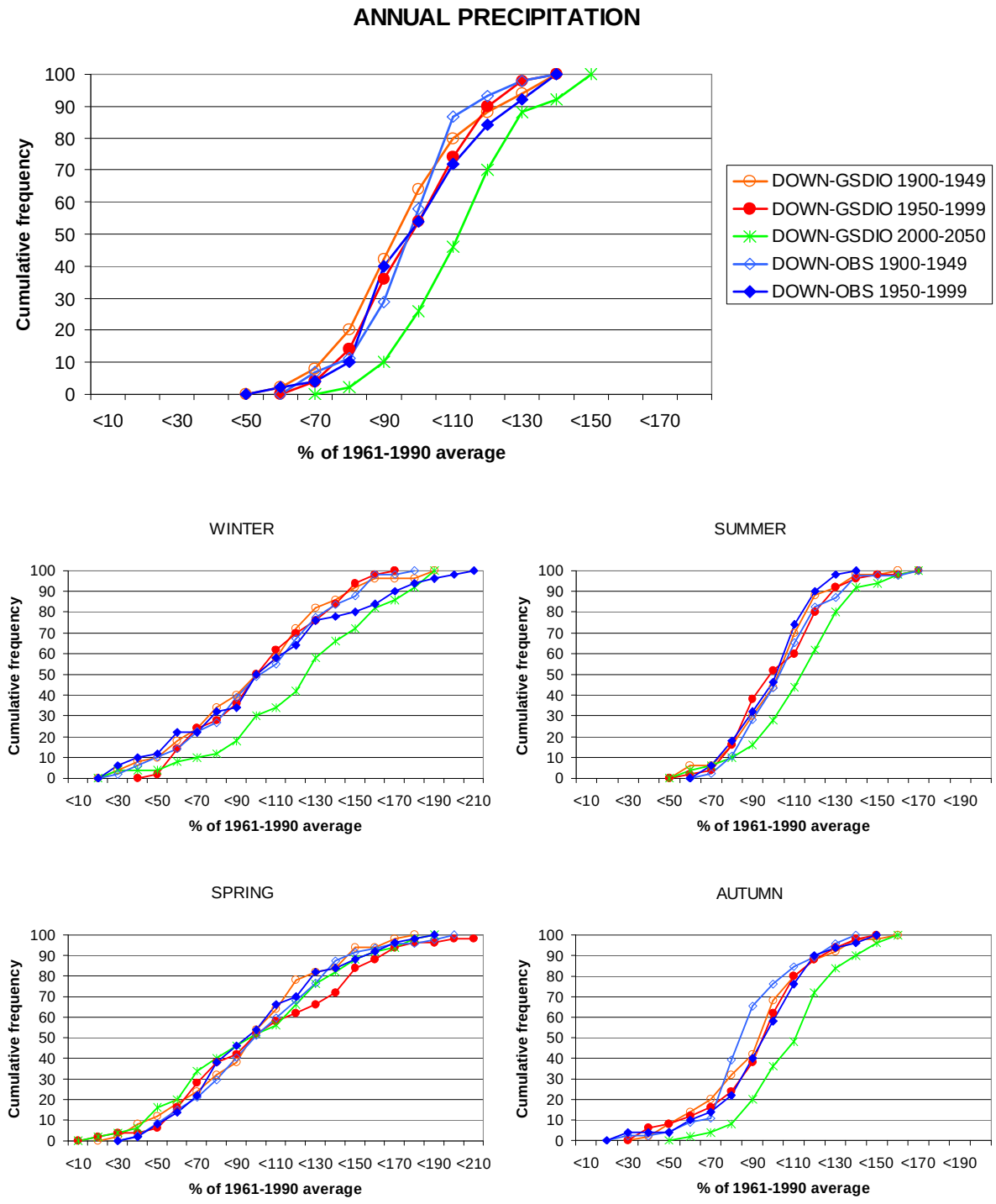

Figure 9. Cumulative frequency distributions of downscaled precipitation during the 20th century from observations (blue) and the GSDIO integration (red) at Samnanger in region 6. Downscaled GSDIO scenario for the period 2000-2049 is also shown (green).

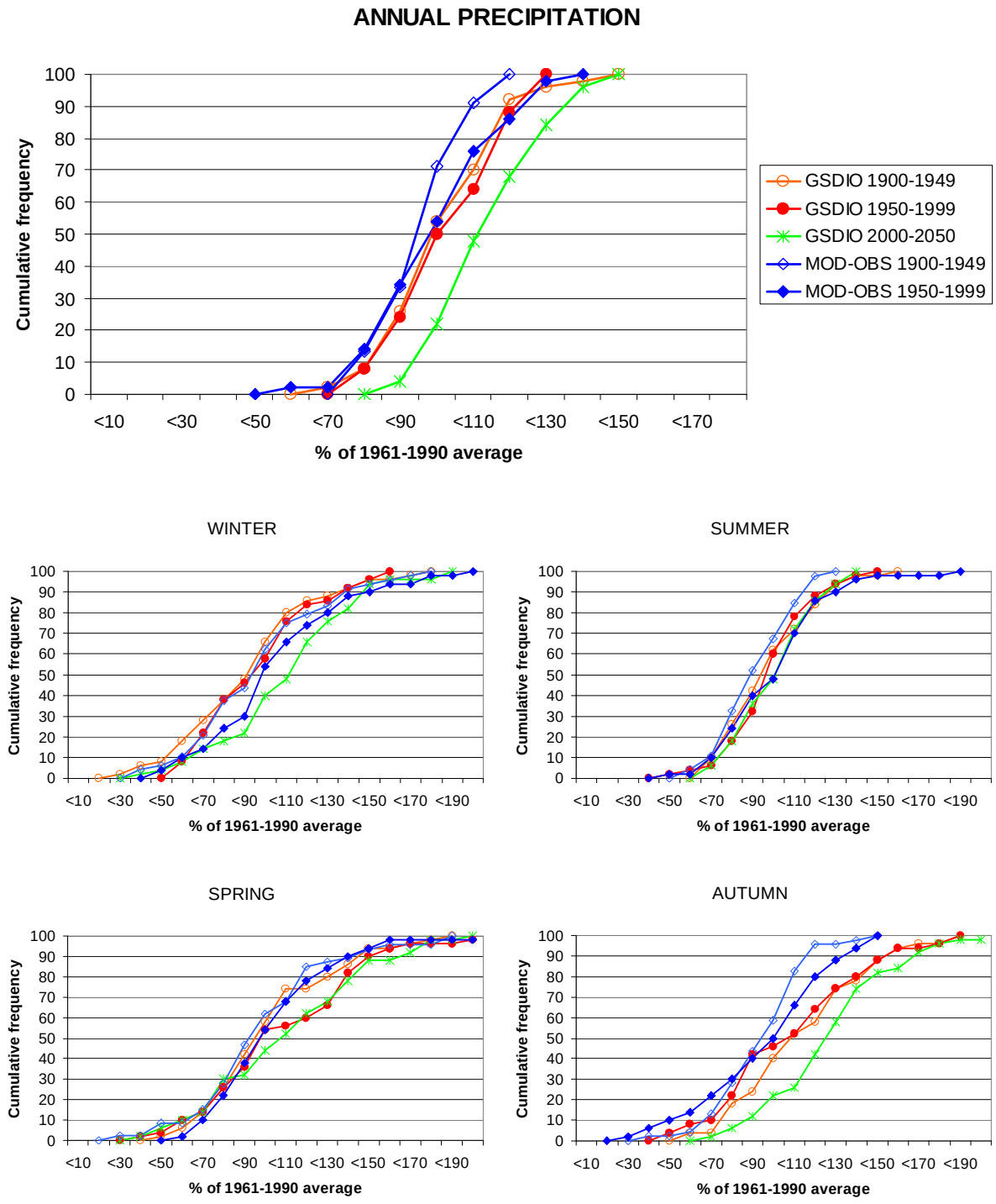

Figure 10. Cumulative frequency distributions of downscaled precipitation during the 20th century from observations (blue) and the GSDIO integration (red) at Bones in region 11. Downscaled GSDIO scenario for the period 2000-2049 is also shown (green).

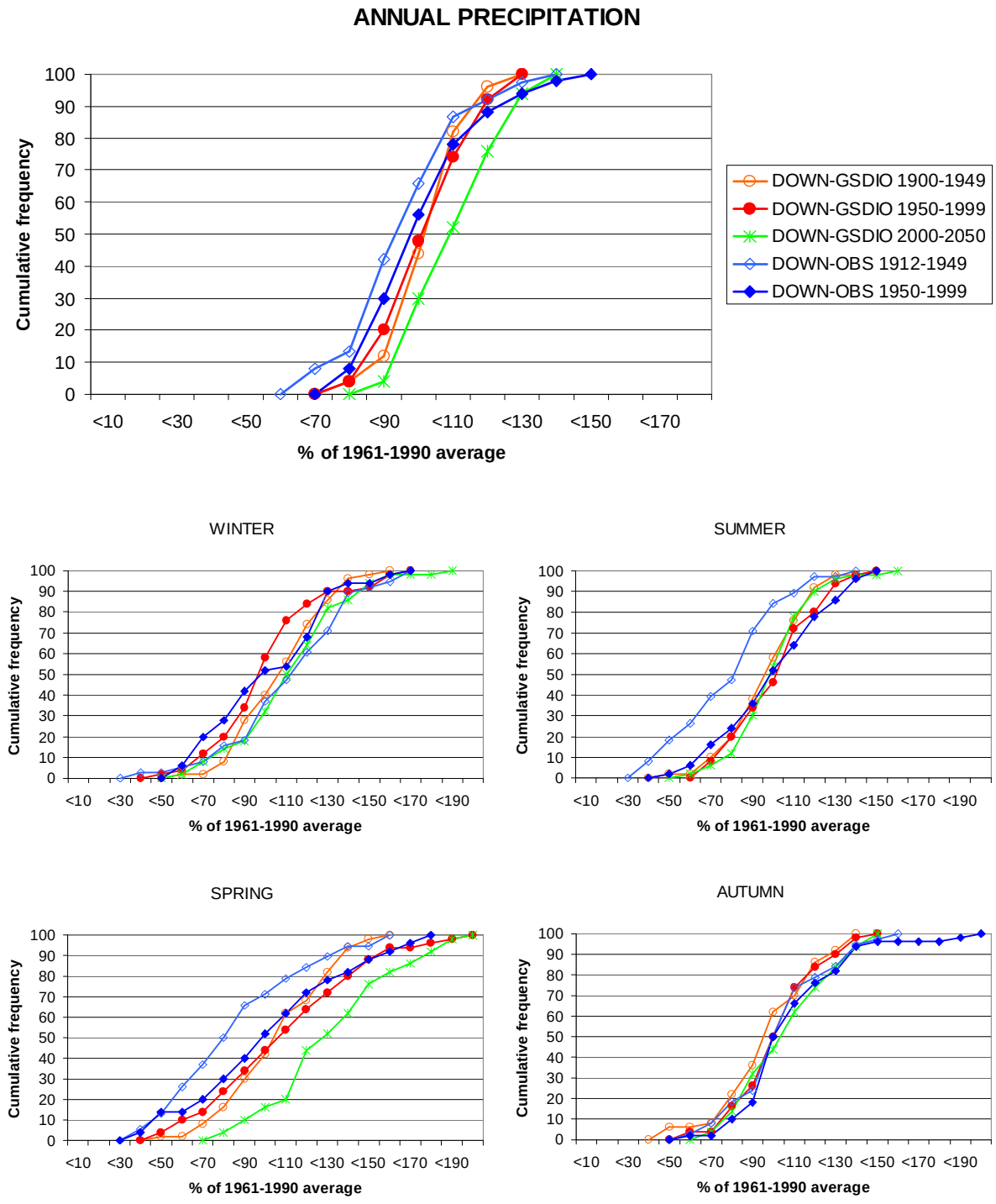

Figure 11. Cumulative frequency distributions of downscaled precipitation during the 20th century from observations (blue) and the GSDIO integration (red) at Svalbard Airport in region 14. Downscaled GSDIO scenario for the period 2000-2049 is also shown (green).

3.2 Change rates for precipitation - definitions

Filtered time series of observed precipitation from 1900 to 2000 and projected precipitation from 1950 to 2050 are shown in figures 12 and 13 for stations in region 2 and 10, respectively. Observed and modelled curves should not be compared on a year-to-year basis.

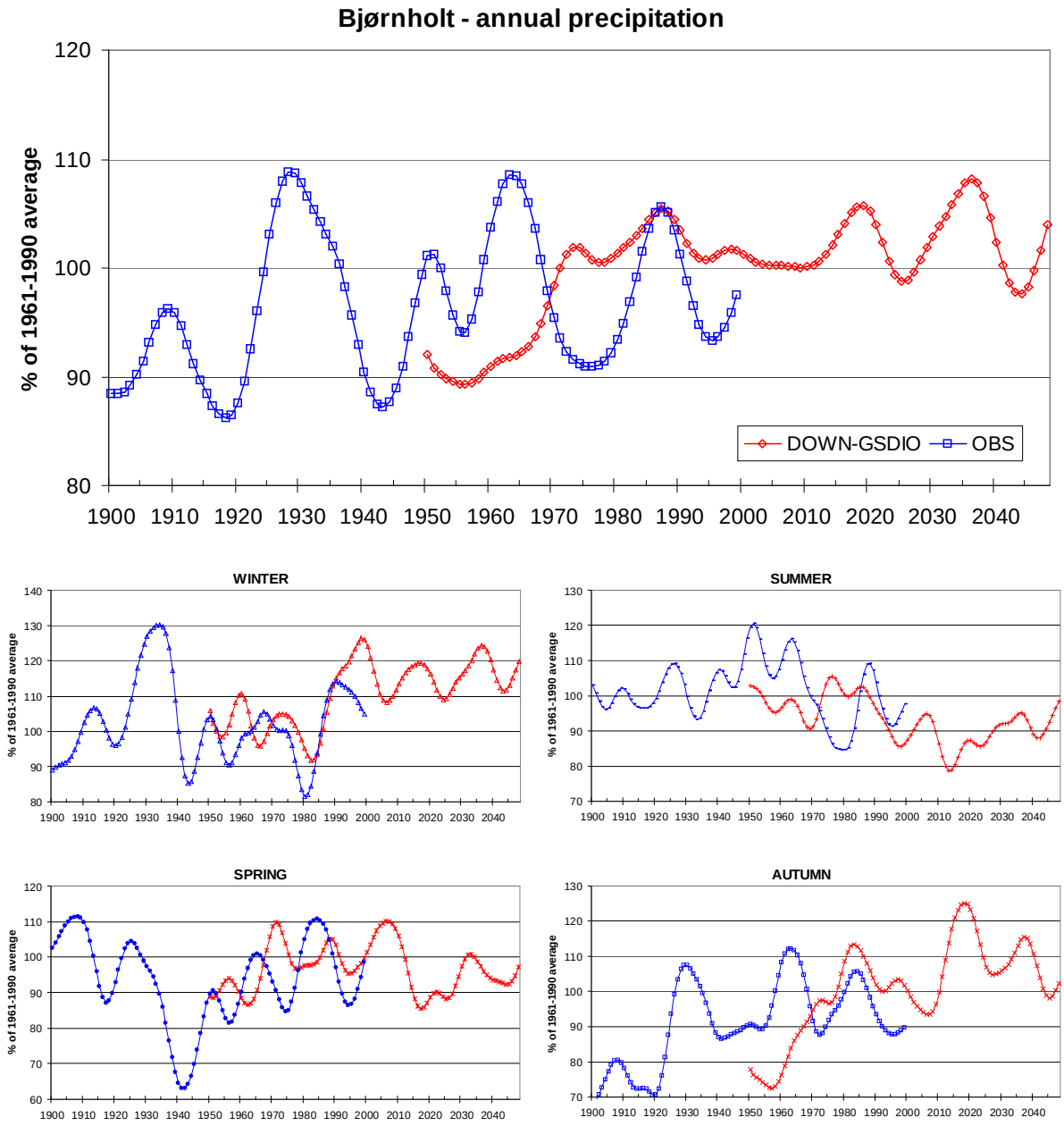

Figure 12. Filtered series of observed (blue) and projected (red)annual and seasonal precipitation at Bjørnholt in region 2.

Even the decadal scale variability is mainly the result of natural variability, and it is thus a matter of chance whether or not observed and modelled variation is in phase. At Drevja (Figure 13) the projected spring precipitation happens to agree remarkably well with the observations during the last 50 years, while this is not the case for winter and autumn precipitation.

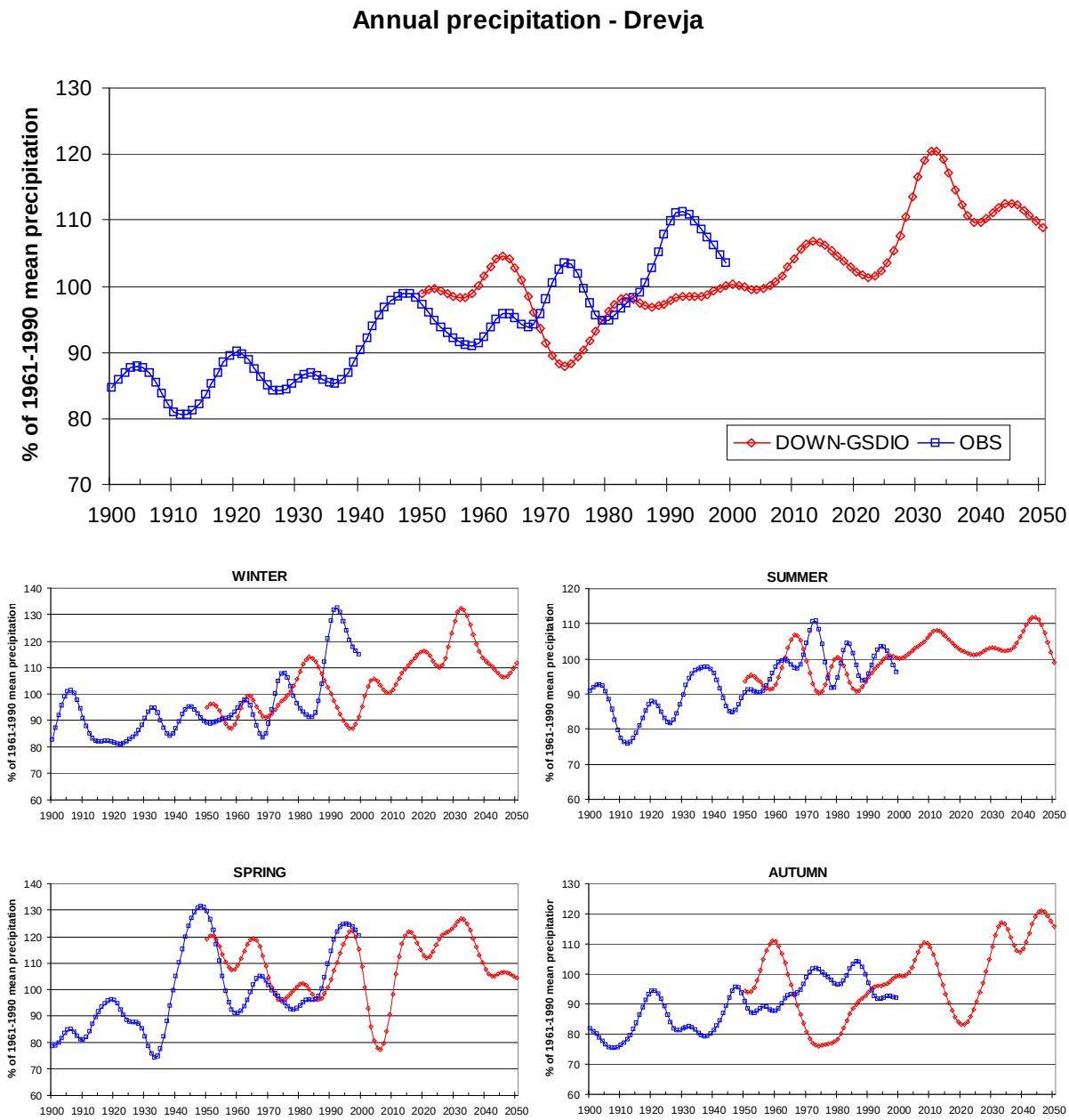

Figure 13.Filtered series of observed (blue) and projected (red)annual and seasonal precipitation at Drevja in region 10.

It is concerning the long-term trends, the scenarios are supposed to have credibility. However, the decadal scale variability makes even these trends sensitive for how they are defined. In the present paper, precipitation trends are defined as the changes from the standard normal period 1961-1990 to the period 2020-2049, and they are given in % of the 1961-1990 average per decade. For the stations in Figure 1, these change rates and their 95% confidence intervals are presented in table A-3 in Appendix. These change rates are also used for producing the maps in section 3.3.

In Table 5, typical change rates for each precipitation region are presented together with the similar change rates achieved by downscaling models using only circulation indices (EOFs from the SLP field) as predictors (cf. section 2.1). These are given to indicate how much of the change which is associated with circulation changes alone.

Table 5. Annual/seasonal precipitation change rates in different regions according to the downscaling models. The "final models" refer to the present downscaling models. The "SLP models" refers to models using only SLP as predictor. Change rates are given ± 95% confidence interval. Unit: % of the 1961-1990 average per decade. Statistically significant changes (5% level) are given in red (positive) or blue (negative).

Region	Model	Annual	Winter	Spring	Summer	Autumn
1	Final	0.4 ± 0.6	**2.9 ± 1.3**	-0.9 ± 1.1	-0.7 ± 0.8	0.8 ± 1.1
	SLP	-0.1 ± 0.6	**1.4 ± 1.2**	**-1.4 ± 1.1**	-0.7 ± 0.8	0.3 ± 1.0
2	Final	0.3 ± 0.6	**2.7 ± 1.3**	-0.8 ± 1.3	**-1.2 ± 1.0**	**1.2 ± 1.2**
	SLP	-0.6 ± 0.7	0.7 ± 1.1	**-1.3 ± 1.3**	**-1.2 ± 1.0**	-0.2 ± 1.1
3	Final	0.6 ± 0.7	**2.9 ± 1.5**	-1.1 ± 1.4	**-1.3 ± 1.2**	**1.3 ± 1.3**
	SLP	-0.3 ± 0.6	**1.6 ± 1.2**	**-1.4 ± 1.4**	**-1.3 ± 1.2**	0.0 ± 1.2
4	Final	**1.3 ± 0.6**	**2.6 ± 1.4**	-1.1 ± 1.5	0.1 ± 0.8	**2.4 ± 0.8**
	SLP	**0.9 ± 0.6**	**1.8 ± 1.4**	-1.1 ± 1.5	0.1 ± 0.8	**1.8 ± 0.8**
5	Final	**1.7 ± 0.7**	**3.2 ± 1.6**	-1.4 ± 1.9	0.2 ± 0.8	**2.9 ± 0.9**
	SLP	**1.2 ± 0.7**	**2.4 ± 1.6**	-1.4 ± 1.9	0.1 ± 0.8	**2.3 ± 0.8**
6	Final	**2.5 ± 0.7**	**3.2 ± 1.7**	-0.4 ± 2.1	**1.7 ± 1.0**	**3.9 ± 1.0**
	SLP	**1.7 ± 0.7**	**2.3 ± 1.7**	-0.7 ± 2.1	**1.2 ± 1.0**	**2.7 ± 0.9**
7	Final	**1.0 ± 0.4**	**2.1 ± 1.0**	0.7 ± 1.0	0.1 ± 0.5	**1.6 ± 0.6**
	SLP	0.4 ± 0.4	**1.2 ± 1.0**	-0.7 ± 0.9	0.1 ± 0.5	**0.6 ± 0.5**
8	Final	**2.2 ± 0.7**	**2.1 ± 1.4**	0.1 ± 1.8	**2.9 ± 1.0**	**3.0 ± 1.2**
	SLP	**1.5 ± 0.7**	**1.2 ± 1.4**	-0.3 ± 1.8	**2.8 ± 1.0**	**1.8 ± 1.2**
9	Final	**2.0 ± 0.6**	**2.5 ± 1.2**	1.3 ± 1.6	**1.7 ± 0.8**	**2.7 ± 1.1**
	SLP	**1.3 ± 0.6**	**1.1 ± 1.2**	0.2 ± 1.5	**1.5 ± 0.8**	**2.1 ± 1.1**
10	Final	**2.4 ± 0.7**	**2.2 ± 1.2**	1.5 ± 2.0	**1.0 ± 1.0**	**4.0 ± 1.2**
	SLP	**1.4 ± 0.7**	**1.2 ± 1.2**	0.2 ± 1.9	**1.0 ± 1.0**	**2.5 ± 1.2**
11	Final	**2.7 ± 0.7**	**2.0 ± 1.3**	**1.9 ± 1.8**	-0.3 ± 1.0	**5.9 ± 1.4**
	SLP	**1.0 ± 0.7**	0.6 ± 1.3	0.7 ± 1.8	-0.3 ± 1.0	**2.2 ± 1.3**
12	Final	**1.4 ± 0.4**	**1.8 ± 0.8**	**2.7 ± 0.9**	0.2 ± 0.6	**2.7 ± 0.8**
	SLP	0.2 ± 0.4	0.3 ± 0.7	**-0.8 ± 0.8**	0.2 ± 0.6	0.7 ± 0.6
13	Final	**1.5 ± 0.4**	**1.8 ± 0.8**	-0.3 ± 0.7	**0.8 ± 0.7**	**3.2 ± 0.8**
	SLP	-0.2 ± 0.4	-0.2 ± 0.8	**-1.2 ± 0.7**	0.6 ± 0.7	0.0 ± 0.7
14	Final	**1.4 ± 0.6**	**1.7 ± 1.2**	**4.6 ± 1.4**	**-0.9 ± 0.9**	0.6 ± 0.9
	SLP	0.4 ± 0.5	0.1 ± 1.1	**3.3 ± 1.4**	**-0.9 ± 0.9**	-0.3 ± 0.9

3.3 Precipitation changes from 1961-1990 to 2020-2049

The empirically downscaled precipitation scenario based upon the GSDIO integration gives an increase in annual mean precipitation all over the country (Fig. 14). The precipitation increase is statistically significant (5% level) in all parts of Norway except the south-eastern regions 1-3 (Table 5). The increase exceeds 2 % per decade in the western and north-western regions 6, 8, 9, 10 and 11. Comparisons with results from downscaling models based only upon SLP indicate that the projected circulation changes alone would also lead to significant precipitation increase in these regions, though the contribution from the temperature dependent term is also considerable. In the northern regions 11-14, the temperature dependent term is the dominant contributor to the projected annual trend.

The projected winter precipitation (Fig. 15) shows statistically significant increase all over the country. The increase is at maximum in the southern regions 1 to 6, where it exceeds 2.5 % per decade. The temperature dependent term is the dominant contributor to the increase in winter precipitation in the 4 northernmost regions. This is also the case in the south-eastern regions 1 and 2, though the circulation changes also give positive contribution here. In the south-western regions 4-6, about ¾ of the projected precipitation increase may be associated with changes in the SLP field.

In spring (Fig. 16), the final models give statistically significant precipitation changes only in regions 11, 12 and 14. In the Arctic region 14, the highly significant precipitation increase is mainly associated with circulation changes, but also the temperature term contributes positively. In the northern mainland regions 11 and 12, the temperature term is the main contributor to the positive trends. In all southern regions statistically insignificant negative trends are found. They are strongly connected to the circulation changes which, without the compensating effect from the temperature term, would have given statistically significant precipitation decrease in the south-eastern regions 1-3.

The projected summer precipitation (Fig. 17) shows statistically significant negative trends in the south-eastern regions 2 and 3, and statistically significant positive trends in regions 6, 8, 9,10 and 13. As temperature is skipped as predictor in most of the downscaling models for summer months, the trends in projected summer precipitation are closely related to changes in the atmospheric circulation.

The final models give increased autumn precipitation all over the country (Fig. 18). The increase is statistically significant in all regions except in region 1 in south-east and the Arctic region 14. In south-eastern and northern regions, the increase is mainly produced by the temperature dependent term. This term also contributes to the projected increase in the western regions, but here the circulation terms contribute even more.

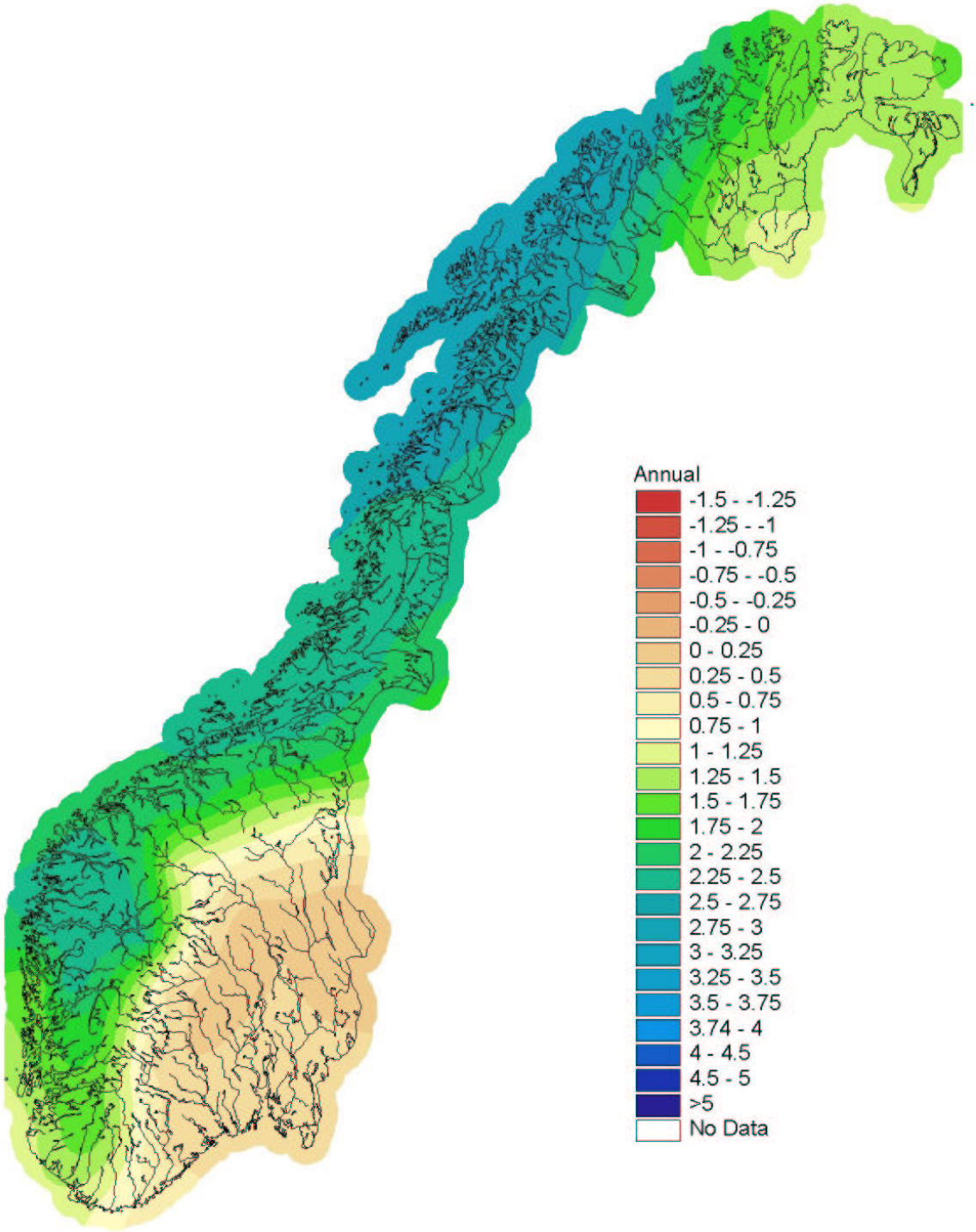

Figure 14. Results from empirical downscaling: Change in annual precipitation from the period 1961-1990 to the period 2021-50. Unit: % of 1961-1990 average per decade.

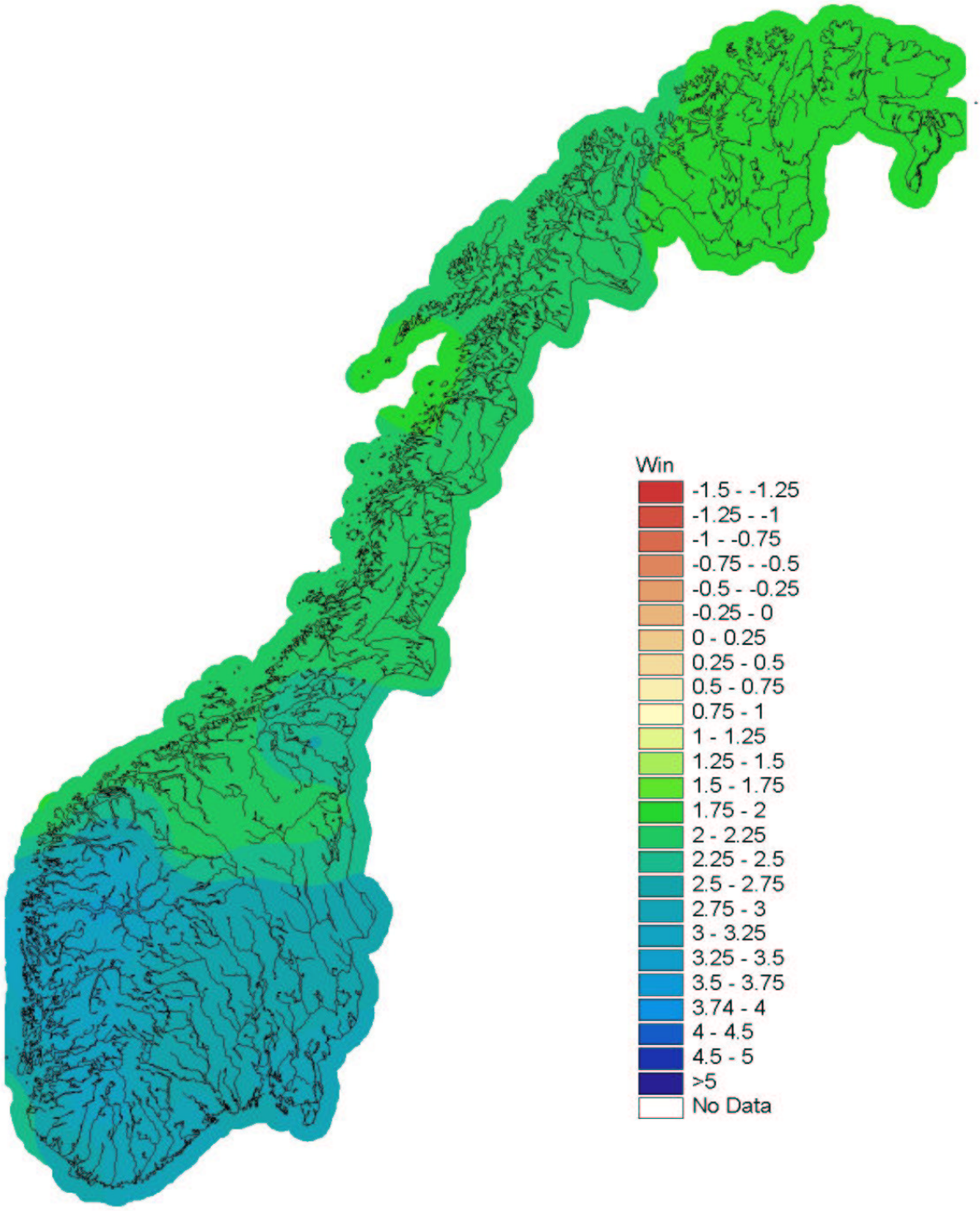

Figure 15. Results from empirical downscaling: Change in winter precipitation (Dec-Jan-Feb) from the period 1961-1990 to the period 2021-50. Unit: % of 1961-1990 average per decade.

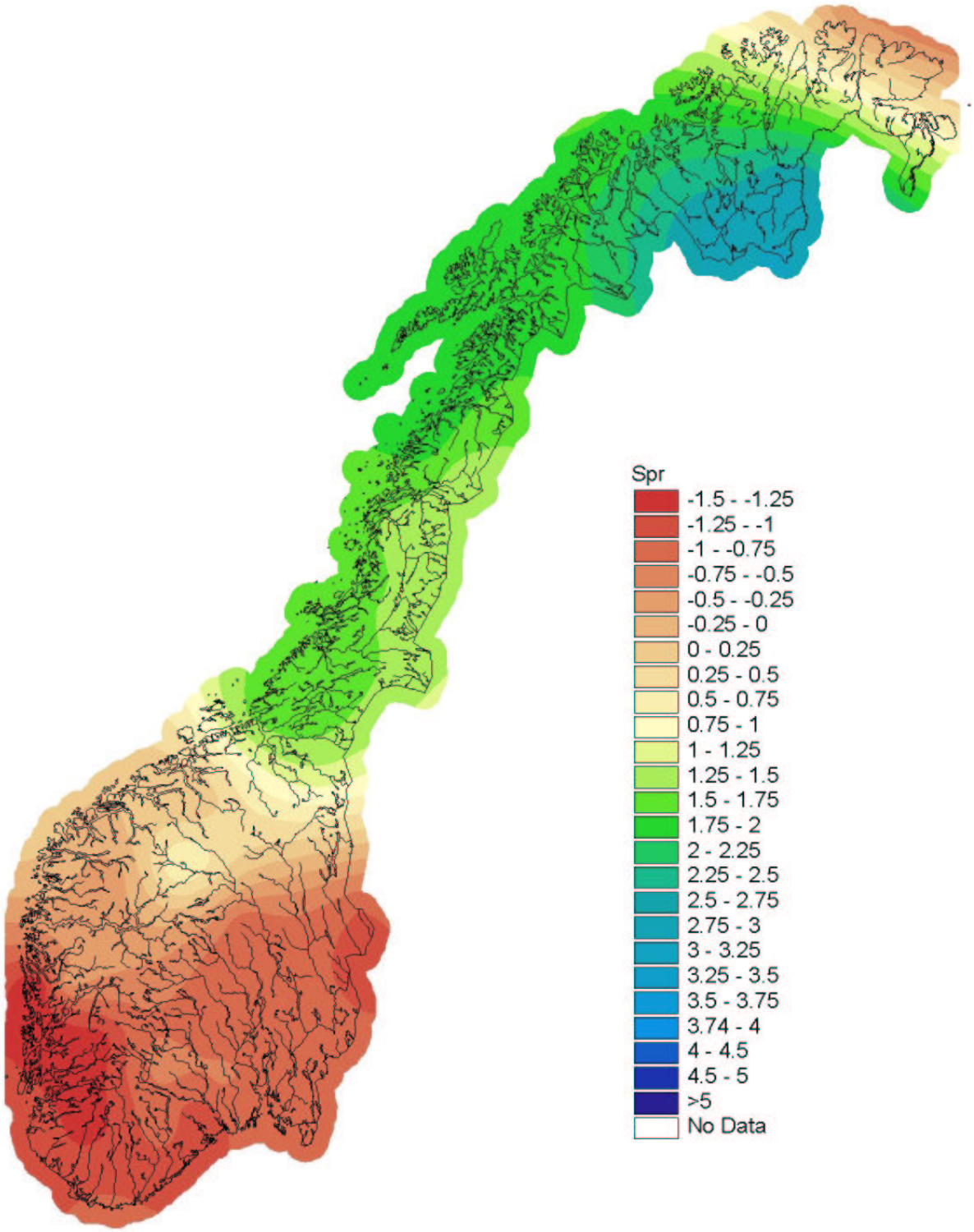

Figure 16. Results from empirical downscaling: Change in winter precipitation (Mar-Apr-May) from the period 1961-1990 to the period 2021-50. Unit: % of 1961-1990 average per decade.

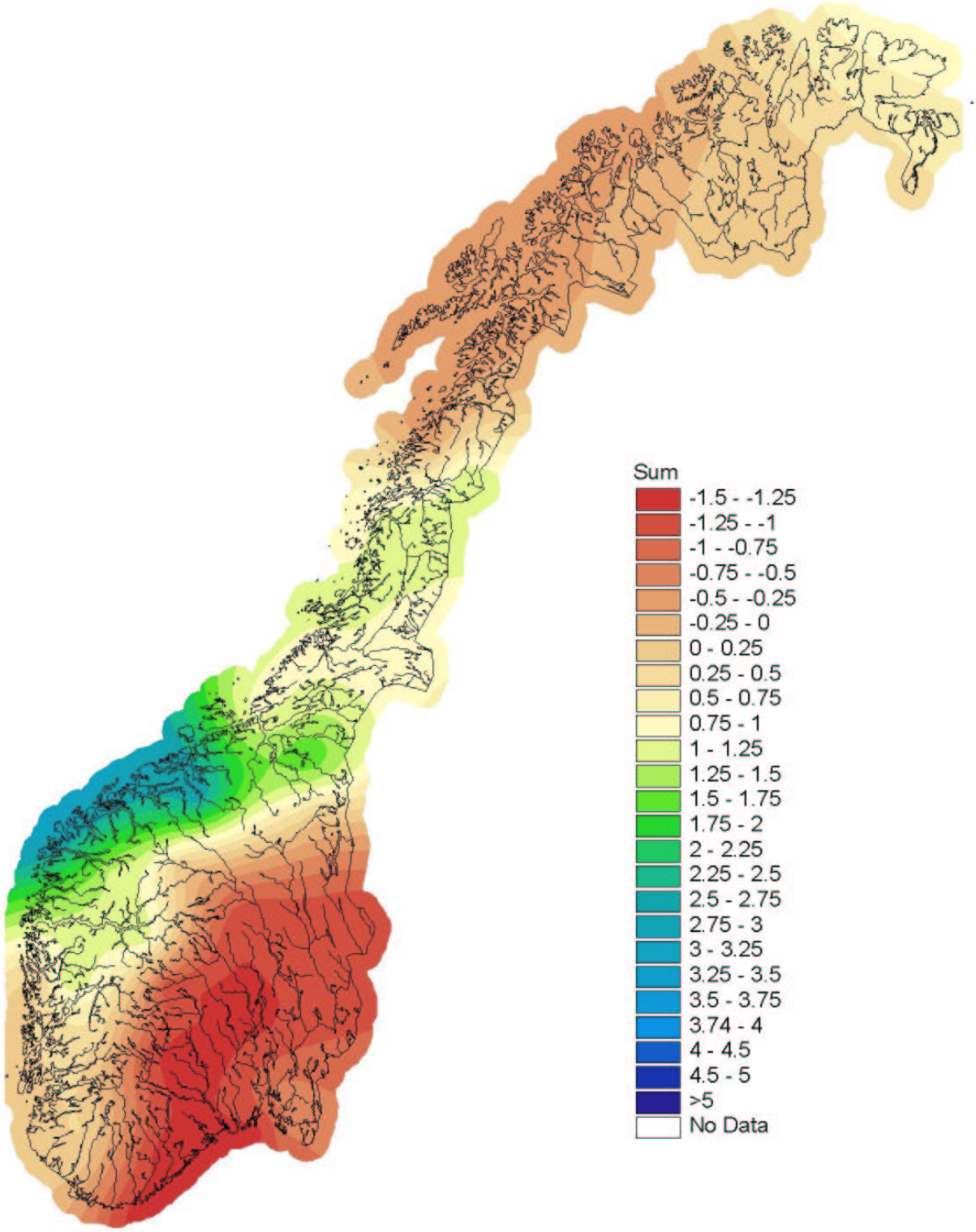

Figure 17. Results from empirical downscaling: Change in winter precipitation (Jun-Jul-Aug) from the period 1961-1990 to the period 2020-49. Unit: % of 1961-1990 average per decade.

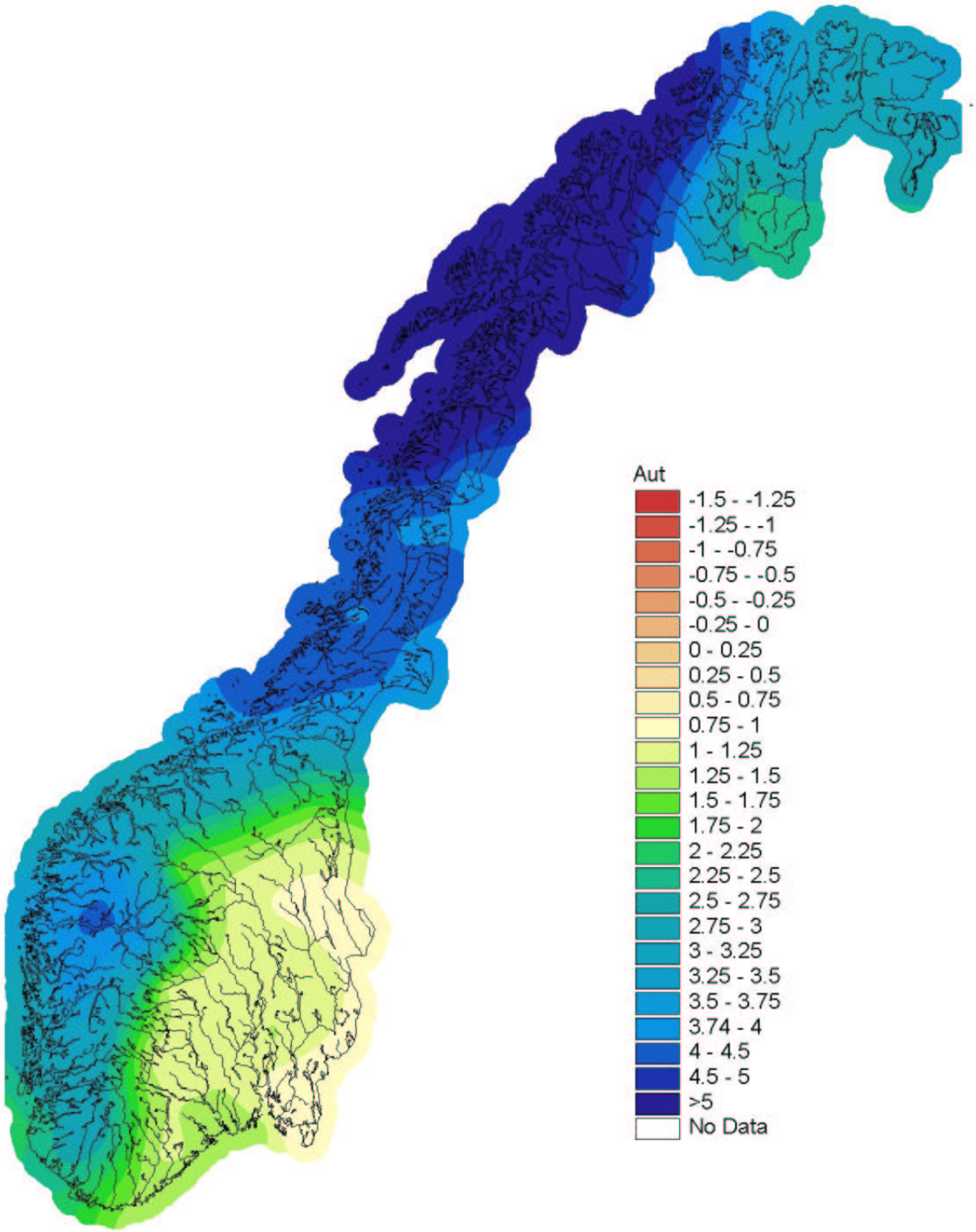

Figure 18. Results from empirical downscaling: Change in winter precipitation (Sep-Oct-Nov) from the period 1961-1990 to the period 2021-50. Unit: % of 1961-1990 average per decade.

4. Comparisons between empirical and dynamical downscaling

Results from dynamical downscaling over Norway of the GSDIO integration were presented by Bjørge et al. (2000). Typical regional precipitation change rates based upon these results are shown in Figure 19 together with results from the present empirical downscaling.

Taken into account the confidence intervals given in Table 5, the only significant disagreements between the results from the dynamical and empirical downscaling, are the changes in summer precipitation in the southern regions. In south-western Norway Bjørge et al. (2000) project a highly significant increase in summer precipitation, while the present study indicates a smaller increase which is statistically significant only in the northern part of the area. In south-eastern Norway Bjørge et al. (2000) projects at average a small increase (though their maps show a decrease in central parts of this area). The present study indicates a significant decrease in most of the area. These discrepancies can to a large degree be attributed to the differences between these investigations concerning definitions of the changes: While the present study is based upon comparisons of the 30-year periods 1961-90 and 2020-49, Bjørge et al. (2000) have compared the 20-year time-slices 1980-99 and 2030-49. Application of these time-slices in the present study would give results more similar to those from the dynamical downscaling.

Still, some of the difference between empirically and dynamically downscaled summer scenarios may be attributed to differences between the methods. The present empirical downscaling method has a clear weakness concerning summer precipitation, as only changes connected to changes in the SLP field are modelled. Wilby and Wigley (2000), however, points out that also dynamical climate models may have problems with modelling summer precipitation: In summer, the correlation between specific humidity and precipitation was stronger in the HadCM2 than in observations. It is not known whether this feature, which probably is the result from oversimplification of the precipitation process, also is valid for ECHAM4, and for the downscaling model “HIRHAM”.

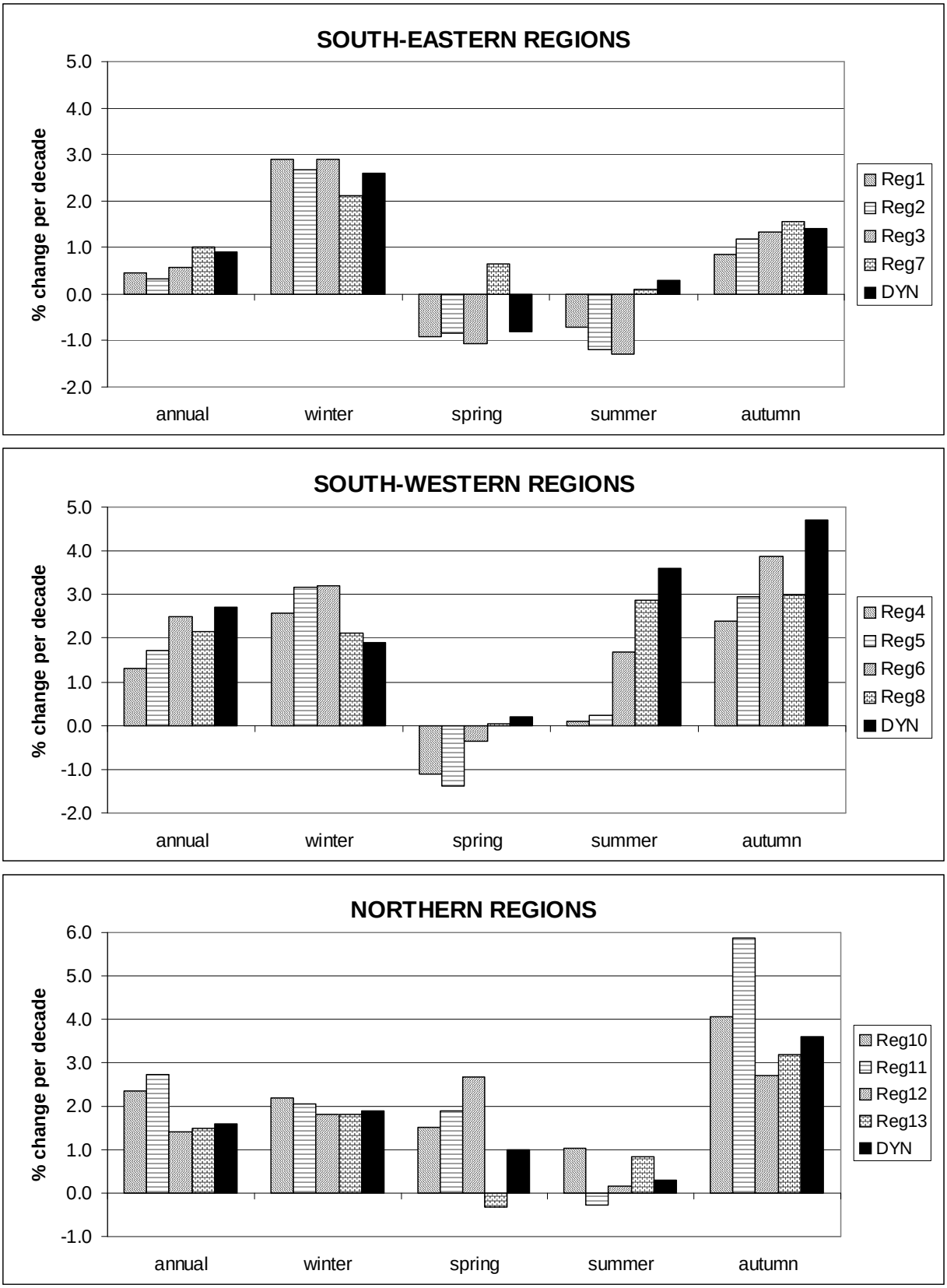

Figure 19. Annual and seasonal precipitation trends up to 2050 resulting from the present analysis and from dynamical downscaling from the same global model. Results from the present study are given for the regions in Figure 1, while results from dynamical downscaling are given only for "south-eastern", "south-western" and "northern" Norway.

5. Summary and conclusions

Empirical downscaling of the ECHAM4/OPYC3 GSDIO integration gives an increase in annual precipitation of 0.3-2.7 % per decade in different Norwegian regions up to 2050. The increase is statistically significant (5% level) in all regions except the south-eastern regions 1-3. In autumn and winter, the precipitation increase is statistically significant almost everywhere. In autumn, the increase exceeds 2.5% per decade in western and northern regions (5-6 and 8-13). In winter, it exceeds 2.5% per decade in the southern regions 1-6. In spring, the precipitation trends tend to be negative in southern Norway and positive in northern Norway. The negative trends are statistically significant in the south-eastern regions 1-3. At Svalbard, projected spring precipitation increases significantly. In summer there is also a negative trend in the precipitation in south-eastern regions, but statistically significant increase in summer precipitation is projected along the west coast of central Norway.

For summer precipitation, only trends connected to changes in the atmospheric circulation are described by the present downscaling models. For the other seasons, it is possible to distinguish between changes attributed to circulation changes and temperature changes, respectively. The positive trends in autumn and winter precipitation are in all regions partly attributed to the temperature increase. Changes in circulation nevertheless accounts for a substantial part of the precipitation increase in the regions where the largest precipitation trends are projected, i.e. in western regions in autumn, and in southern regions during winter. In spring, circulation induced changes are dominating the modelled precipitation changes in southern Norway, while the temperature term gives significant contributions to the precipitation increase in northern regions. Generally, the circulation dependent terms contribute to increase the regional differences, especially between east and west in autumn, and between south and north in winter and spring.

A relevant question is whether there is any difference in the credibility connected to the precipitation trends which are attributed to changes in temperature and circulation, respectively. It may seem as if the regional temperature signals from different climate models are more consistent than changes in regional circulation indices like the NAO index (e.g. Benestad 2000, Räisänen 2001). Nevertheless, Hanssen-Bauer and Førland (2001) found that the GSDIO integration actually shows a quite realistic intensification of the westerly wind-field over Norway during the latest decades. Besides, the connection between circulation indices and precipitation is probably more robust than the connection between temperature and precipitation. We thus conclude that further investigations are needed to judge the credibility of the different parts of the modelled trends.

There is generally good agreement between results from empirical and dynamical downscaling. Significant differences are found in summer, when the dynamical downscaling gives larger areas with increasing precipitation than the present empirical downscaling gives.

References

Benestad, R.E., 2000: Future Climate Scenarios for Norway based on linear empirical downscaling and inferred directly from AOGCM results. DNMI Report 23/00 KLIMA, Norwegian Meteorological Institute, Oslo, Norway.

Benestad, R.E., 2001: A comparison between two empirical downscaling strategies. (in press) *Int. J. Climatol*.

Benestad, R.E., I. Hanssen-Bauer, I., E.J. Førland, O.E. Tveito and K. Iden, 1999: Evaluation of monthly mean data fields from the ECHAM4/OPYC3 control integration. DNMI Report 14/99 KLIMA, Norwegian Meteorological Institute, Oslo, Norway.

Bjørge, D., J.E. Haugen and T.E. Nordeng, 2000: Future Climate in Norway. Dynamical downscaling experiments within the RegClim project. Research Report 103, Norwegian Meteorological Institute, Oslo, Norway.

Christensen, O.B., J.H. Christensen, B. Machenhauer & M. Botzet, 1998: Very high-resolution regional climate simulations over Scandinavia – Present climate. *J.Climate*, **11,** 3204-3229.

Crane and Hewitson 1998: Doubled CO_2 precipitation changes for the Susquehanna Basin: downscaling from the GENESIS General Circulation Model. *Int. J. Climatol*., **18**, 65-76

Hanssen-Bauer, I. and E.J. Førland 1998: Long-term trends in precipitation and temperature in the Norwegian Arctic: can they be explained by changes in atmospheric circulation patterns? *Climate Research,* **10**, 143-153.

Hanssen-Bauer, I. and E.J. Førland 2000: Temperature and precipitation variations in Norway and their links to atmospheric circulation. *Int. J. Climatol* ,**20**, No. 14, 1693-1708.

Hanssen-Bauer, I. and E.J. Førland 2001: Verification and analysis of a climate simulation of temperature and pressure fields over Norway and Svalbard. *Climate Research,* **16**, 225-235.

Hanssen-Bauer, I. and P.Ø. Nordli 1998: Annual and seasonal temperature variations in Norway 1876-1997. DNMI Report 25/98 KLIMA, Norwegian Meteorological Institute, Oslo, Norway.

Hanssen-Bauer, I, O.E. Tveito and E.J. Førland 2000: Temperature scenarios for Norway. Empirical downscaling from ECHAM4/OPYC3. DNMI-KLIMA 24/00, 53 pp.

Hewitson, B.C. and R.G. Crane, 1996: Climate downscaling: Techniques and application, *Clim. Res.*, **7**, 85-95

Huth, R., J. Kyselý & L. Pokorná, 2000: A GCM simulation of heat waves, dry spells, and their relationships to circulation. *Clim.Change*, **46,** 29-60.

IPCC (International Panel on Climate Change), 2001: *Climate Change 2001: The Scientific Basis*. Contribution of Working Group I to the Third Assessment Report of IPCC. [J.T Houghton, Y. Ding, D.J. Griggs, M. Nouger, P.J. van der Linden, X. Dai, K. Maskell, C.A. Johnson (eds.)] ISBN 0 521 01495 6, Cambridge University Press, Cambridge, UK, and New York, NY, USA, 881 pp. (Available at *www.ipcc.ch*)

Iversen, T., E.J. Førland, L.P. Røed and F. Stordal, 1997: Regional Climate Under Global Warming. Project Description. NILU, P.O.Box 100, N-2007 Kjeller, Norway.

Murphy J., 1999: An evaluation of statistical and dynamical techniques for downscaling local climate. *J. Climate,* **12**, 2256-2284.

Räisänen, J., 2001: CO2-Induced Climate Change in CMIP2 Experiments: Quantification of Agreement and Role of Internal Variability. *J. Climate,* **14**, 2088-2104

Roeckner, E., K. Arpe, L. Bengtsson, M. Christof, M. Claussen, L. Dümenil, M. Esch, M. Giorgetta, U. Schlese & U. Schulzweida, 1996: The atmospheric general circulation model ECHAM4: Model description and simulation of present-day climate. Report No. 218, Max-Planck-Institut für Meteorologie, Hamburg, Germany

Roeckner, E., L. Bengtsson, J. Feichter, J. Lelieveld & H. Rohde, 1998: Transient climate change simulations with a coupled atmosphere-ocean GCM including the tropospheric sulphur cycle. Report No. 266, Max-Planck-Institut für Meteorologie, Hamburg, Germany

Roeckner, E., L. Bengtsson, J. Feichter, J. Lelieveld & H. Rodhe, 1999: Transient climate change simulations with a coupled atmosphere-ocean GCM including the tropospheric sulphur cycle, *J.Climate*, **12**, 3004-3032.

Zorita, E. and H. von Storch, 1997: A survey of statistical downscaling techniques. GKSS97/E/20, 42pp.

Zorita, E. and H. von Storch, 1999: A survey of statistical downscaling techniques. *J.Climate* (in press)

Zorita, E., J.P. Hughes, D.P. Lettenmaier and H. von Storch, 1995: Stochastic Characterization of Regional Circulation Patterns for Climate Model Diagnosis and Estimation of Local Precipitation. *J.Climate*, **8**, 1023-1042.

Wilby, R.L. and Wigley T.M.L., 1997: Downscaling general circulation model output: a review of methods and limitations. *Prog. Phys. Geography*, **21**, 530-548

Wilby, R.L. and Wigley T.M.L., 2000: Precipitation predictors for downscaling: Observed and general circulation model relationships. *Int. J. Climatol.*, **20**, 641-661

Wilby R.L., L.E. Hay and G.H. Leavesley, 1999: A comparison of downscaled and raw GCM output: implications for climate change scenarios in the San Juan River basin, Colorado. *J. Hydrology*, 225 67-71

APPENDIX – 1

Table A1. Basic information for stations used in the present paper: Number and name, geographical coordinates and precipitation region(Fig. 2).

ST. NO.	ST. NAME	LATITUDE	LONGITUDE	REGION
01080	HVALER	59° 02'	11° 02'	1
01230	HALDEN	59° 07'	11° 23'	1
01650	STRØMSFOSS SLUSE	59° 18'	11° 40'	1
03450	HAGA I EIDSBERG	59° 32'	11° 18'	1
17150	RYGGE	59° 23'	10° 47'	1
00060	LINNES	61° 34'	12° 30'	2
05350	NORD-ODAL	60° 23'	11° 33'	2
11900	BIRI	60° 57'	10° 36'	2
13100	VESTRE GAUSDAL	61° 21'	9° 46'	2
18500	BJØRNHOLT I NORDMARKA	60° 03'	10° 41'	2
22950	NORD-AURDAL II	60° 55'	9° 25'	2
25640	GEILO	60° 32'	8° 10'	2
27500	FERDER FYR	59° 02'	10° 32'	2
28920	VEGGLI	60° 15'	8° 42'	2
30370	BESSTUL I GJERPEN	59° 27'	9° 32'	2
33250	RAULAND	59° 42'	8° 02'	2
37230	TVEITSUND	59° 02'	8° 31'	2
34600	DRANGEDAL	59° 06'	9° 04'	3
36200	TORUNGEN FYR	58° 24'	8° 48'	3
38600	MYKLAND	58° 38'	8° 17'	3
39100	OKSØY FYR	58° 04'	8° 03'	3
42720	BAKKE	58° 25'	6° 40'	4
43360	EGERSUND	58° 27'	6° 00'	4
44800	SVILAND	58° 49'	5° 55'	4
47300	UTSIRA FYR	59° 18'	4° 53'	4
42890	SKREÅDALEN	58° 49'	6° 43'	5
46050	ULLA	59° 23'	6° 32'	5
46450	RØLDAL	59° 50'	6° 50'	5
50540	BERGEN - FLORIDA	60° 23'	5° 20'	5
50350	SAMNANGER	60° 28'	5° 54'	6
54130	LÆRDAL - TØNJUM	61° 04'	7° 31'	6
56320	LAVIK	61° 07'	5° 33'	6
58320	MYKLEBUST I BREIM	61° 43'	6° 37'	6
10400	RØROS	62° 34'	11° 23'	7
15660	SKJÅK	61° 54'	8° 10'	7
59100	KRÅKENES FYR	62° 02'	4° 59'	8
62480	ONA II	62° 52'	6° 32'	8
63100	ØKSENDAL	62° 41'	8° 25'	8
68330	LIEN I SELBU	63° 13'	11° 07'	9
70850	SKJÆKERFOSSEN	63° 50'	12° 01'	10
71550	ØRLAND III	63° 42'	9° 36'	10
75100	LIAFOSS	64° 50'	11° 57'	10
77850	SUSENDAL	65° 22'	14° 16'	10
78100	DREVJA	65° 60'	13° 25'	10
79740	DUNDERLANDSDALEN	66° 30'	14° 54'	10
80700	GLOMFJORD	66° 49'	13° 59'	11
83500	KRÅKMO	67° 48'	15° 59'	11
86850	BARKESTAD	68° 49'	14° 48'	11
88100	BONES I BARDU	68° 39'	18° 15'	11
90450	TROMSØ	69° 39'	18° 56'	11
92700	LOPPA	70° 20'	21° 28'	11
93300	SUOLOVUOPMI	69° 35'	23° 32'	12
93700	KAUTOKEINO	69° 01'	23° 03'	12
97250	KARASJOK	69° 28'	25° 31'	12
96400	SLETNES FYR	71° 05'	28° 13'	13
98550	VARDØ	70° 22'	31° 05'	13
99840	SVALBARD LUFTHAVN	78° 16'	15° 29'	14
99910	NY-ÅLESUND II	78° 56'	11° 57'	14

APPENDIX – 2

Table A2. Observed and modelled means and standard deviations of monthly mean precipitation (%). a) Bjørnholt, region 2.

SEASONAL MEAN PRECIPITATION (% OF OBSERVED 1961-1990 MEAN)					
DATA	PERIOD	WINTER	SPRING	SUMMER	AUTUMN
OBS	1901-1930	102	101	102	82
	1931-1960	105	80	105	92
	1961-1990	100	100	100	100
DOWNSC. FROM OBS	1901-1930	112	105	110	89
	1931-1960	111	86	110	103
	1961-1990	100	100	100	100
DOWNSC. FROM GSDIO	1901-1930	106	101	92	91
	1931-1960	110	92	100	83
	1961-1990	100	101	100	100
	1991-2020	118	97	88	106
	2021-2050	116	96	92	108
STANDARD DEVIATION OF SEASONAL PRECIPITATION (% OF OBSERVED 1961-1990 MEAN)					
DATA	PERIOD	WINTER	SPRING	SUMMER	AUTUMN
OBS	1901-1930	44	31	28	32
	1931-1960	46	33	38	29
	1961-1990	41	35	34	36
DOWNSC. FROM OBS	1901-1930	30	21	32	30
	1931-1960	36	20	33	27
	1961-1990	29	25	27	25
DOWNSC. FROM GSDIO	1901-1930	35	23	25	27
	1931-1960	27	28	22	29
	1961-1990	31	31	23	29
	1991-2020	27	22	21	25
	2021-2050	26	24	23	23

Table A2 b) Samnanger, region 6.

SEASONAL MEAN PRECIPITATION (% OF OBSERVED 1961-1990 MEAN)					
DATA	PERIOD	WINTER	SPRING	SUMMER	AUTUMN
OBS	1901-1930	108	101	91	79
	1931-1960	96	93	99	86
	1961-1990	99	100	100	100
DOWNSC. FROM OBS	1901-1930	112	103	109	86
	1931-1960	98	91	103	91
	1961-1990	99	100	100	100
DOWNSC. FROM GSDIO	1901-1930	98	88	96	99
	1931-1960	95	95	92	93
	1961-1990	100	100	100	100
	1991-2020	110	87	93	109
	2021-2050	120	91	102	117
STANDARD DEVIATION OF SEASONAL PRECIPITATION (% OF OBSERVED 1961-1990 MEAN)					
DATA	PERIOD	WINTER	SPRING	SUMMER	AUTUMN
OBS	1901-1930	30	35	23	22
	1931-1960	33	38	23	29
	1961-1990	40	41	30	26
DOWNSC. FROM OBS	1901-1930	26	33	16	24
	1931-1960	30	31	16	27
	1961-1990	43	36	18	19
DOWNSC. FROM GSDIO	1901-1930	36	36	15	23
	1931-1960	31	27	16	24
	1961-1990	30	43	16	19
	1991-2020	30	39	16	19
	2021-2050	41	39	18	18

Table A2 c) Bones, region 11.

SEASONAL MEAN PRECIPITATION (% OF OBSERVED 1961-1990 MEAN)					
DATA	PERIOD	WINTER	SPRING	SUMMER	AUTUMN
OBS	1901-1930	92	103	77	91
	1931-1960	99	121	88	87
	1961-1990	100	100	100	100
DOWNSC. FROM OBS	1901-1930	88	87	87	89
	1931-1960	96	108	89	93
	1961-1990	100	100	100	100
DOWNSC. FROM GSDIO	1901-1930	89	91	101	113
	1931-1960	89	115	90	116
	1961-1990	100	100	99	100
	1991-2020	97	109	101	120
	2021-2050	113	111	97	129
STANDARD DEVIATION OF SEASONAL PRECIPITATION (% OF OBSERVED 1961-1990 MEAN)					
DATA	PERIOD	WINTER	SPRING	SUMMER	AUTUMN
OBS	1901-1930	33	42	18	24
	1931-1960	43	49	20	31
	1961-1990	37	33	33	37
DOWNSC. FROM OBS	1901-1930	35	28	18	16
	1931-1960	32	32	19	27
	1961-1990	31	31	19	30
DOWNSC. FROM GSDIO	1901-1930	36	22	21	34
	1931-1960	27	39	20	31
	1961-1990	27	40	21	28
	1991-2020	29	33	17	32
	2021-2050	33	40	20	31

Table A2 d) Svalbard Airport, region 14.

SEASONAL MEAN PRECIPITATION (% OF OBSERVED 1961-1990 MEAN)					
DATA	PERIOD	WINTER	SPRING	SUMMER	AUTUMN
OBS	1901-1930	103	84	56	76
	1931-1960	101	76	91	114
	1961-1990	100	100	100	100
DOWNSC. FROM OBS	1901-1930	112	86	67	95
	1931-1960	107	92	88	111
	1961-1990	100	100	100	100
DOWNSC. FROM GSDIO	1901-1930	106	104	98	96
	1931-1960	99	114	93	99
	1961-1990	100	100	100	100
	1991-2020	109	129	103	102
	2021-2050	110	124	95	104
STANDARD DEVIATION OF SEASONAL PRECIPITATION (% OF OBSERVED 1961-1990 MEAN)					
DATA	PERIOD	WINTER	SPRING	SUMMER	AUTUMN
OBS	1901-1930	55	64	27	20
	1931-1960	50	28	34	41
	1961-1990	40	46	44	30
DOWNSC. FROM OBS	1901-1930	23	38	22	24
	1931-1960	32	30	25	18
	1961-1990	25	38	22	20
DOWNSC. FROM GSDIO	1901-1930	23	24	19	21
	1931-1960	23	34	19	22
	1961-1990	25	32	22	19
	1991-2020	24	36	21	26
	2021-2050	28	30	14	19

APPENDIX – 3

Table A3. Annual/seasonal precipitation change from 1961-90 to 2020-49 with 95% confidence intervals. Unit: % of 1961-1990 average per decade. Statistical significant changes are given in bold.

Region	Station	Annual	Winter	Spring	Summer	Autumn
1	1080	0.46 ± 0.57	**2.87** ± 1.29	-0.94 ± 1.11	-0.73 ± 0.84	0.90 ± 1.07
	1230	0.47 ± 0.56	**2.93** ± 1.28	-0.91 ± 1.10	-0.71 ± 0.84	0.86 ± 1.06
	1650	0.43 ± 0.56	**2.93** ± 1.28	-0.93 ± 1.10	-0.72 ± 0.84	0.80 ± 1.05
	3450	0.42 ± 0.56	**2.92** ± 1.28	-0.89 ± 1.10	-0.72 ± 0.84	0.82 ± 1.06
	17150	0.47 ± 0.56	**2.91** ± 1.28	-0.86 ± 1.10	-0.72 ± 0.85	0.85 ± 1.06
2	60	0.10 ± 0.60	**2.61** ± 1.30	-0.98 ± 1.37	**-1.14** ± 1.01	**0.93** ± 1.14
	5350	0.26 ± 0.59	**2.66** ± 1.29	-0.93 ± 1.32	**-1.16** ± 1.02	**1.11** ± 1.14
	11900	0.25 ± 0.60	**2.69** ± 1.28	-0.91 ± 1.34	**-1.18** ± 1.02	**1.17** ± 1.15
	13100	0.17 ± 0.61	**2.72** ± 1.28	-0.88 ± 1.39	**-1.16** ± 1.02	**1.13** ± 1.15
	18500	0.42 ± 0.59	**2.64** ± 1.30	-0.82 ± 1.28	**-1.19** ± 1.03	**1.25** ± 1.15
	22950	0.18 ± 0.60	**2.68** ± 1.29	-0.88 ± 1.39	**-1.13** ± 1.01	**1.19** ± 1.15
	25640	0.46 ± 0.59	**2.65** ± 1.30	-0.66 ± 1.30	**-1.15** ± 1.01	**1.26** ± 1.16
	27500	0.49 ± 0.61	**2.65** ± 1.29	-0.81 ± 1.29	**-1.25** ± 1.05	**1.35** ± 1.16
	28920	0.26 ± 0.60	**2.77** ± 1.26	-0.87 ± 1.36	**-1.15** ± 1.01	**1.15** ± 1.15
	30370	0.44 ± 0.60	**2.69** ± 1.28	-0.77 ± 1.29	**-1.24** ± 1.05	**1.26** ± 1.16
	33250	0.46 ± 0.59	**2.74** ± 1.27	-0.70 ± 1.31	**-1.17** ± 1.02	**1.21** ± 1.15
	37230	0.43 ± 0.61	**2.75** ± 1.27	-0.86 ± 1.34	**-1.24** ± 1.05	**1.23** ± 1.15
3	34600	0.41 ± 0.70	**2.79** ± 1.52	-1.18 ± 1.38	**-1.27** ± 1.23	**1.34** ± 1.30
	36200	0.59 ± 0.70	**2.92** ± 1.50	-1.05 ± 1.38	**-1.29** ± 1.23	**1.34** ± 1.30
	38600	0.58 ± 0.70	**2.98** ± 1.48	-1.03 ± 1.38	**-1.27** ± 1.22	**1.30** ± 1.30
	39100	0.72 ± 0.72	**2.93** ± 1.49	-0.99 ± 1.38	**-1.34** ± 1.25	**1.41** ± 1.32
4	42720	**1.38** ± 0.56	**2.58** ± 1.37	-1.07 ± 1.43	0.10 ± 0.85	**2.44** ± 0.80
	43360	**1.28** ± 0.56	**2.58** ± 1.38	-1.12 ± 1.45	0.12 ± 0.84	**2.41** ± 0.80
	44800	**1.30** ± 0.55	**2.56** ± 1.38	-1.10 ± 1.46	0.13 ± 0.84	**2.37** ± 0.80
	47300	**1.26** ± 0.56	**2.58** ± 1.37	-1.17 ± 1.46	0.09 ± 0.85	**2.38** ± 0.80
5	42890	**1.71** ± 0.68	**3.17** ± 1.56	-1.34 ± 1.87	0.24 ± 0.77	**2.96** ± 0.86
	46050	**1.73** ± 0.69	**3.16** ± 1.56	-1.38 ± 1.96	0.24 ± 0.76	**2.96** ± 0.86
	46450	**1.79** ± 0.69	**3.17** ± 1.56	-1.38 ± 1.94	0.25 ± 0.76	**2.94** ± 0.86
	50540	**1.62** ± 0.67	**3.16** ± 1.56	-1.39 ± 1.91	0.24 ± 0.76	**2.91** ± 0.86
6	50350	**2.44** ± 0.76	**3.18** ± 1.69	-0.36 ± 2.14	**1.66** ± 1.03	**3.86** ± 0.99
	54130	**2.49** ± 0.68	**3.19** ± 1.70	-0.34 ± 2.00	**1.73** ± 1.04	**3.82** ± 0.99
	56320	**2.49** ± 0.75	**3.19** ± 1.69	-0.34 ± 2.16	**1.71** ± 1.02	**3.87** ± 0.99
	58320	**2.51** ± 0.74	**3.18** ± 1.69	-0.36 ± 2.13	**1.70** ± 1.03	**3.87** ± 0.99
7	10400	**0.93** ± 0.42	**2.13** ± 0.98	0.58 ± 0.92	0.09 ± 0.53	**1.50** ± 0.57
	15660	**1.07** ± 0.41	**2.13** ± 0.97	0.73 ± 0.98	0.10 ± 0.53	**1.64** ± 0.61
8	59100	**2.21** ± 0.71	**2.07** ± 1.43	0.07 ± 1.83	**3.01** ± 0.98	**2.99** ± 1.24
	62480	**2.17** ± 0.72	**2.15** ± 1.42	0.06 ± 1.85	**2.95** ± 0.98	**2.94** ± 1.25
	63100	**2.10** ± 0.70	**2.13** ± 1.42	0.05 ± 1.85	**2.70** ± 0.93	**2.99** ± 1.24
9	68330	**2.04** ± 0.60	**2.52** ± 1.21	1.32 ± 1.60	**1.67** ± 0.84	**2.70** ± 1.08
10	70850	**2.27** ± 0.66	**2.20** ± 1.24	1.54 ± 1.94	0.92 ± 1.00	**4.08** ± 1.21
	71550	**2.40** ± 0.68	**2.21** ± 1.23	1.57 ± 1.94	0.98 ± 1.00	**4.05** ± 1.20
	75100	**2.36** ± 0.71	**2.19** ± 1.24	1.54 ± 2.01	**1.04** ± 1.00	**4.00** ± 1.20
	77850	**2.33** ± 0.67	**2.14** ± 1.26	1.47 ± 1.97	**1.03** ± 1.00	**4.14** ± 1.20
	78100	**2.41** ± 0.72	**2.16** ± 1.26	1.48 ± 2.02	**1.07** ± 1.01	**4.02** ± 1.19
	79740	**2.39** ± 0.70	**2.16** ± 1.25	1.41 ± 2.04	**1.07** ± 1.00	**3.96** ± 1.19
11	80700	**2.84** ± 0.70	**2.01** ± 1.36	**1.87** ± 1.85	-0.28 ± 0.96	**5.99** ± 1.39
	83500	**2.68** ± 0.69	**2.03** ± 1.36	1.81 ± 1.84	-0.28 ± 0.95	**5.66** ± 1.38
	86850	**2.79** ± 0.70	**2.05** ± 1.35	**1.93** ± 1.84	-0.28 ± 0.94	**5.77** ± 1.37
	88100	**2.65** ± 0.67	**2.08** ± 1.34	**1.91** ± 1.82	-0.28 ± 0.96	**5.88** ± 1.38
	90450	**2.83** ± 0.69	**2.06** ± 1.34	**1.94** ± 1.83	-0.28 ± 0.95	**5.93** ± 1.38
	92700	**2.63** ± 0.67	**2.04** ± 1.33	**1.96** ± 1.78	-0.27 ± 0.95	**5.90** ± 1.39
12	93300	**1.47** ± 0.37	**1.79** ± 0.82	**2.43** ± 0.89	0.17 ± 0.58	**2.69** ± 0.75
	93700	**1.35** ± 0.41	**1.87** ± 0.83	**2.89** ± 0.86	0.17 ± 0.60	**2.72** ± 0.82
	97250	**1.39** ± 0.39	**1.77** ± 0.83	**2.73** ± 0.87	0.17 ± 0.60	**2.73** ± 0.78
13	96400	**1.43** ± 0.41	**1.80** ± 0.77	-0.32 ± 0.71	**0.83** ± 0.72	**3.00** ± 0.81
	98550	**1.54** ± 0.41	**1.80** ± 0.78	-0.32 ± 0.71	**0.87** ± 0.72	**3.35** ± 0.83
14	99840	**1.37** ± 0.55	**1.65** ± 1.19	**4.60** ± 1.45	-0.90 ± 0.92	0.61 ± 0.87
	99910	**1.52** ± 0.56	**1.72** ± 1.20	**4.60** ± 1.37	-0.86 ± 0.95	0.58 ± 0.87